ANALYSIS OF POWER TRANSMISSION IN HIGH STEP-UP DC-DC CONVERTER

A THESIS SUBMITTED TO THE GRADUATE SCHOOL OF APPLIED SCIENCES OF NEAR EAST UNIVERSITY

By
ALAA MUDHAFAR ABDULLAH ABDULLAH

In Partial Fulfilment of the Requirements for the Degree of Master of Science in Electrical and Electronic Engineering

NICOSIA, 2020

ALAA MUDHAFAR ABDULLAH ABDULLAH

ANALYSIS OF POWER TRANSMISSION IN HIGH STE-UP DC-DC CONVERTER

NEU 2020

ANALYSIS OF POWER TRANSMISSION IN HIGH STEP-UP DC-DC CONVERTER

A THESIS SUBMITTED TO THE GRADUATE SCHOOL OF APPLIED SCIENCES OF NEAR EAST UNIVERSITY

By
ALAA MUDHAFAR ABDULLAH ABDULLAH

In Partial Fulfilment of the Requirements for the Degree of Master of Science in Electrical and Electronic Engineering

NICOSIA, 2020

ALAA MUDHAFAR ABDULLAH ABDULLAH: ANALYSIS OF POWER TRANSMISSION IN HIGH STEP-UP DC-DC CONVERTER

Approval of Director of Graduate School of Applied Sciences

Prof. Dr. Nadire CAVUS

We certify this thesis is satisfactory for the award of the degree of Master of Science in Electrical and Electronic Engineering

Examining Committee in Charge:

Prof. Dr. Ebrahim Babaei	Supervisor, Department of Electrical and Computer Engineering, University of Tabriz – Iran
Assist. Prof. Dr. Parvaneh Esmaili	Department of Electrical and Electronic Engineering, NEU
Assist. Prof. Dr. Lida Ebrahimi Vafaei	Department of Mechanical Engineering, NEU

I hereby declare that all information in this document has been obtained and presented in accordance with academic rules and ethical conduct. I also declare that, as required by these rules and conduct, I have fully cited and referenced all material and results that are not original to this work.

Name, Last name: ALAA MUDHAFAR ABDULLAH ABDULLAH

Signature:

Date:

ACKNOWLEDGEMENTS

First, I would like to show my appreciation to my research supervisor, Prof. Dr. Ebrahim Babaei, Near East University, Northern Cyprus, for his help and guidance throughout my research. My profound gratitude goes to the head of electrical engineering department, Prof. Dr. Bulent Bilgehan. Also, to all my lecturers in the department and other non-teaching staff. I would also like to thank my family and friends especially my parent for their support.

To my family…

ABSTRACT

This thesis has presented the analysis of power transmission in high step-up dc/dc converter. The analysis is performed on Non-isolated converters because of their suitability to many applications. The structure and principle of operation of the selected converter circuits are thoroughly discussed. Steady-state analysis of the converters has been performed in both current CCM and DCM, establishing their voltage gain equations. An important property; boundary condition between the CCM and DCM is also determined. For the sake of performance comparison, classical boost converter is used as benchmark, and the result indicated that the converter circuit I and circuit II increased the voltage gain by 60% and 140% respectively. Simulation technique is used to model the converters so as to validate the theoretical results. PSCAD/ EMTDC-V4.2 is used in this thesis for the simulation. This is a robust software that gives insights and deep understanding of the power electronic circuit. The simulation results show that the theoretical values obtain for the various voltages and currents are the same as those obtained from the simulation. Which further ascertained the effectiveness and accuracy of the analysis.

Keywords: Step-up dc/dc converter; power transmission; steady-state analysis, CCM; DCM

ÖZET

Bu tez, yüksek kademeli dc / dc dönüştürücülerdeki güç aktarımının analizini sunmaktadır. Analiz, birçok uygulamaya uygun olmaları nedeniyle izole edilmemiş dönüştürücüler üzerinde gerçekleştirilir. Seçilen dönüştürücü devrelerinin yapısı ve çalışma prensibi ayrıntılı olarak ele alınmıştır. Dönüştürücülerin sürekli durum analizi, hem mevcut CCM hem de DCM'de voltaj kazanç denklemlerini belirleyerek gerçekleştirilmiştir. Önemli bir özellik; CCM ve DCM arasındaki sınır koşulu da belirlenir. Performans karşılaştırması amacıyla, standart güçlendirme dönüştürücü, referans olarak kullanılır ve sonuç, dönüştürücü devre I ve devre II'nin voltaj kazancını sırasıyla% 60 ve% 140 arttırdığını göstermiştir. Teorik sonuçları doğrulayacak şekilde dönüştürücüleri modellemek için simülasyon tekniği kullanılmıştır. Bu tez çalışmasında simülasyonda PSCAD / EMTDC-V4.2 kullanılmıştır. Bu, güç elektroniği devresi hakkında derinlemesine bilgi ve anlayış sağlayan güçlü bir yazılımdır. Simülasyon sonuçları, çeşitli gerilimler ve akımlar için elde edilen teorik değerlerin simülasyondan elde edilenlerle aynı olduğunu göstermektedir. Bu da analizin etkililiğini ve doğruluğunu tespit etti.

Anahtar Kelimeler: Yükseltme dc/dc dönüştürücü; güç iletimi; kararlı durum analizi, CCM; DCM

TABLE OF CONTENTS

CHAPTER 4: CONCLUSION AND FUTURE WORK

LIST OF TABLES

LIST OF FIGURES

LIST OF ABBREVIATIONS

AC:	Alternating Current
DC:	Direct Current
BJT:	Bipolar Junctions Transistor
EMI:	Electromagnetic Interference
PWM:	Pulse Width Modulation
IBC:	Isolated Boost Converter
NIBC:	Non-isolated Boost Converter
VFBC:	Voltage-fed Boost Converter
CFBC:	Current-fed Boost Converter
UBC:	Unidirectional Boost Converter
BBC:	Bidirectional Boost Converter
HSBC:	Hard-switching Boost Converter
SSBC:	Soft-switching Boost Converter
CCM:	Continuous Conduction Mode
DCM:	Discontinuous Conduction Mode
BCM:	Boundary Condition Mode
PSCAD:	Power System Computer Aided Design

CHAPTER 1

INTRODUCTION

1.1 Introduction

Several applications request the use of power electronics converters to provide a suitable power supply for various equipment. Converters are usually used as an interface to condition or transform electric power supply to a required form suitable for the specific user loads. Depending on the type of input and output (alternative current (ac) or direct current (dc)) they operate on, power converter circuits may be categorized as either ac/ac or dc/dc or ac/dc or ac/ac converter. Therefore, power converters that transform dc input signal at certain voltage level to higher/lower voltage-level are called dc/dc converters. Depending on level of output-voltage, they are categorized as either buck or boost or buck/boost. Boost dc converters as the name implies, they converter a given input signal at certain voltage level to a higher voltage level. Similarly, buck dc converters also called step down because they convert a given input voltage into a lower value. A buck-boost converter performs both operations depending on the switching duty ratio.

Recently, converters that can guarantee large voltage ratio has become the basic requirement of step-up dc converter for several modern equipment. These applications generally include fuel cells, servo-motor drives, automobile high-intensity-discharge (HID) lamps, computer systems power supply, uninterrupted power supply (UPS) and X-ray power generators, to mention some (Ismail, Al-Saffar, Sabzali, & Fardoun, 2008). Specifically, for internet service equipment used in telecom the dc-buses operate on approximately 380 V, yet available battery usually has 48 V capacity which means step-up converter having very large voltage ratio is necessary. From theoretical perspectives, it’s possible to satisfy the specifications using step-up converter with very high duty-ratio (Bryant & Kazimierczuk, 2007; D. D. C. Lu, Lee, & Cheng, 2003; X. Wu, Zhang, Ye, & Qian, 2008).

However, in practical situations, the ESR of inductors, active switches, capacitors and semiconductor diode rectifies impose certain constrain on the voltage gain. Furthermore, operating with large duty cycle ratios leads to reverse recovery issues. In the literature, numerous converter structures have been introduced in attempt to produce sufficient output voltage deprived of the necessity of very large duty-ratio (Lin & Hsieh, 2007; Papanikolaou & Tatakis, 2004; Tseng & Liang, 2004; C. M. Wang, 2008; T. F. Wu, Lai, Hung, & Chen, 2008). A flyback dc converter topology has electrical isolation and simple structure in addition to very large output voltage, yet, use of a transformer in this topology leads to increased voltage-stress across the switches.

Some techniques with energy regeneration have been presented to recycle leakage inductance stored energy and therefore alleviate the problem of high voltage-stress across power switches (Lin & Hsieh, 2007; Papanikolaou & Tatakis, 2004; C. M. Wang, 2008). Additionally, coupled-inductor based topologies offer viable solutions to improve the efficiency and get high voltage, while minimizing voltage stress of semiconductor switch

Literature surveys also shows abundant transformer-less step-up dc converters, including the popular quadratic type step-up (Henrique et al., 2005), cascade type step-up (Huber & Jovanovic, 2000), voltage multiplier type (B Axelrod & Berkovich, 2003; Zhou, Pietkiewicz, & Cuk, 1999), and voltage-lift type (Gules & Franco, 2003; Luo, 2001; Luo & Ye, 2004). Fig. 1.1 shows the structure of one of the recently introduced transformer-less step-up converter designed on the basis of switching inductor method (Boris Axelrod, Berkovich, & Ioinovici, 2008). This converter topology uses only one active switch which makes the structure very simple. Notwithstanding, there are still two major issues; voltage of semiconductor switches is same value as output voltage, also, about two and three power components appear along the flow way at time of switchin on and switch-off respectively.

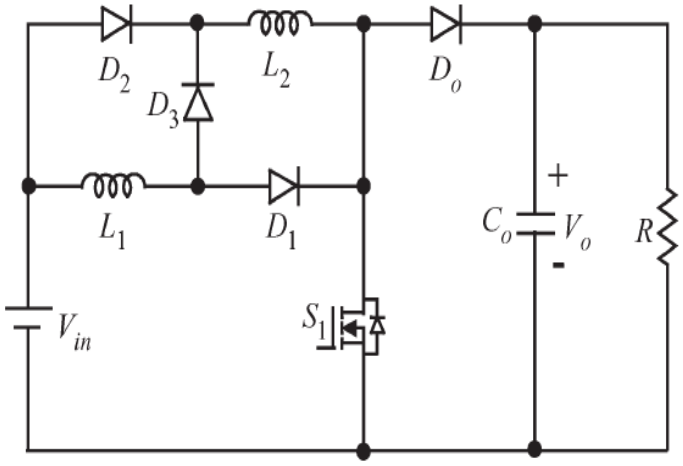

Figure 1.1: Transformerless dc/dc converter introduced in (Boris Axelrod et al., 2008)

1.2 Main Objectives

Major aim of this work is conducting a comprehensive analysis of power transmission in step-up dc/dc converter. Two transformer-less step-up dc/dc converters are used as case study. Following objectives will be considered:

- Power circuit structure and operation principle
- Analysis of converter circuit I in CCM and DCM
- Analysis of converter circuit II in CCM and DCM
- Performance comparison with a classical boost converter
- Converter circuit simulation using PSCAD software

1.3 Significance of the study

For getting a high output-voltage majority of existing step-up converter circuits are complex and expensive. For this purpose, transformer-less step-up converters, that guarantees high voltage gain with relatively low costs and reduced circuit complexity are discussed in this thesis. If we compare with converter topology displayed in Fig. 1.1, the converter circuit I offer a number of advantages: reduced switch voltage-stress, to a value lower than output-voltage, single power-device appears along the flow path at the time of switch-off and only two power-devices during the switch-off. These and many other important properties have been investigated. The simulation will provide a clear insight into the converter circuits' performance and visualization. Simulation models provide safe and efficient solutions to real-world applications and can, therefore, be used to study the potential applications of the converters.

1.4 Scope and Limitations

In this thesis, the practical application is investigated through a simulation modelling of the converters. Hence, no real-world experiment or prototype. However, the results obtained from the simulation is satisfactory. Furthermore, for convenience, certain assumptions are made to simplify the analysis. Viz: converter circuit are in their ideal form, active switches' ON resistance RDS_{ON}, Inductors and capacitors $ESRs$ and diodes' forward voltage drop are neglected and finally, the capacitor is large enough so that its voltage is considered to be constant.

1.5 Structure of the Thesis

Chapter 1: This chapter gives a general introduction on the thesis topic including the background knowledge on power electronics converters, the thesis objectives, significance, scope, limitations and the thesis structure.

Chapter 2: Provides a comprehensive review on boost dc converter structures, starting with conventional and other structures found in existing literature.

Chapter 3: Presents the power circuit description, steady-state analysis, performance comparison and simulation results.

Chapter 4: Conclusion and Future Work.

CHAPTER 2

LITERATURE REVIEW

2.1 Introduction

The main function of dc/dc converter circuits is to change voltage level of an input signal to another voltage level. Step-up (also known as boost) dc/dc converters produces an output voltage larger than input voltage level. The conversions are performed by saving low voltage -input temporarily and at that time discharging it to load. The energy is stored within electric field storing element (capacitors) and/or magnetic field storing devices (inductors) using several diodes and power active switches. The availability and performance of these converter structure have been significantly improved when semiconductor switches were introduced through several manufacturing technologies. Research on step-up converters was promoted by the increase in telecommunication and aerospace companies, with aim of finding optimal weight, power density and efficiency, for a lot of applications (Wilson, 1992). The efficiency has been significantly improved with the advent of field effect transistors (FET) in 1980s. This is because of the fact that, FETs can switch effectively at high frequency than bipolar junction transistors (BJTs), While reducing the drive circuit complexity and switching losses (Jahns & Dai, 2017).

The popular switched mode boost dc/dc converters came in to been after the development of PWM step-up converters. PWM converters are the basic structure of boost converters because of the fact that they possess many important attributes which make them suitable for several applications including low, medium and high power applications. PWM boost converters generally have small number of circuit elements, which make it easier for design, modelling, simulation and implementation. Moreover, because of the presence of inductor at their input, they operate both in CCM and DCM. CCM is referred to converter operation in which the inductor current do not stay at zero during the switching cycles. While DCM refers to the situation when the inductor current reaches and stay at zero for some interval within the operation cycle. Both methods are desirable depending on the application specifications.

On the other hand, PWM boost converter has many deficiencies, such as limited voltage conversion ratio (gain) at reasonable switch duty ratio; less efficiency cause by voltage stresses across the switches and severe reverse recovery; little power-density, which affect their operation in applications that need high power and voltage. Hence, there is clear need to improve the design of conventional step-up converters particularly in applications where high voltage gain, efficiency, power density together with better stability are necessary. Moreover, improvements were made in handling electromagnetic-interference (EMI), cost and ripples in the input signals (Chung, Hui, & Tse, 1998; Jovanović, 1998; Middlebrook, 1988; Williams, 2013).

In this regard, this chapter present a concise review on the major improvements made in design of boost converter, as found in recent literatures. The converter topologies are grouped based on whether they have electrical isolation or not; as isolated boost (IBC) and Non-isolated boost (NIBC) dc/dc converters. Other classifications are current fed boost (CFBC) and voltage fed boost (VFBC) converters, depending on the input circuitry; unidirectional boost (UBC) and Bi-Directional boost converters (BBC), depending on the allowable current flow directions. And finally, hard-switching boost (HSBC) and soft-switching boost converters (SSBC) converters depending on the switching techniques. Figure 2.1 shows the overall classification of the step-up converters adapted in this chapter.

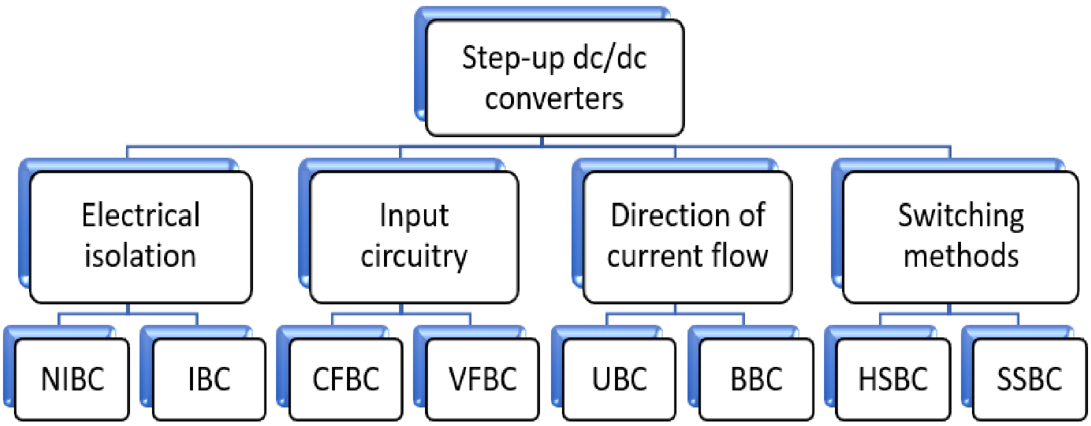

Figure 2.1: Step-up dc/dc converter classification

2.2 NIB dc/dc Converter

As stated in the introduction, the fundamental structure for stepping up dc voltage is PWM step-up dc converters, which is built with three main circuit components viz: switch, diode, and inductor. The overall view of Non-isolated boost dc converter together with PWM step-up converter having common ground between input and output are shown in Fig. 2.2 and Fig. 2.3 respectively. PWM dc converter generally has simple structure, low cost and power Non-isolated boost dc/dc converters suitable for several applications. Like PWM step-up converters Non-isolated dc/dc converter topologies are characterized with minimal weight, cost, size and power levels. Because of this peculiarities and increased demand many researches have been conducted to improve their performance (Choi & Cho, 2002; Duarte & Barbi, 1997; C. Wang, 2006).

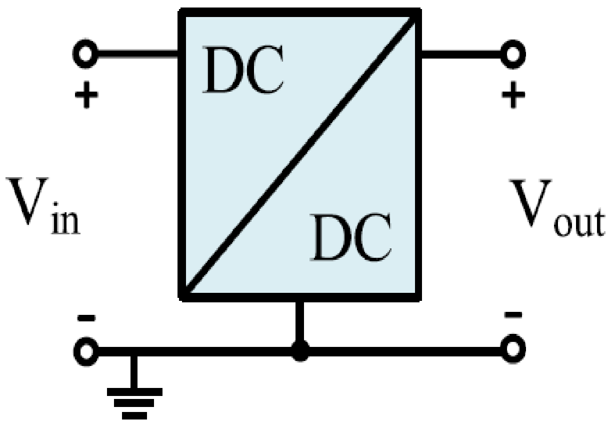

Figure 2.2: Common ground NI dc/dc converter

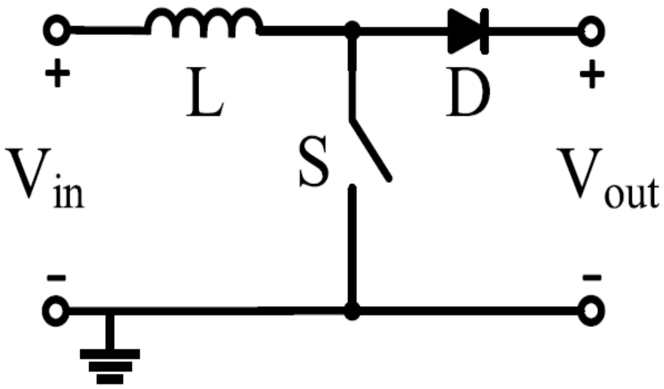

Figure 2.3: PWM step-up converter

These converters can be configured having common ground between input-output as shown in Fig. 2.2 or having a floated output as shown in Fig. 2.4. For applications like grid-connected PV cells where no transformer is needed, using common ground between input and output will enhance the performance of the system. However, the output can be floated in applications where there is no need for sharing ground between the source and the load, like the structure used in 3-level step-up converter proposed in (Zhang, Jiang, Lee, & Jovanovic, 1995). In addition, magnetic coupling can be used in Non-isolated step-up dc/dc converter. This is suitable in applications involving high power systems where high voltage conversion ratio is desired. The incorporation of magnetic coupling in such systems will improve both the reliability and efficiency. Moreover, excluding magnetic coupling in applications where high voltage gain and efficiency is not the key point is a common practice. By eliminating the need for magnetic coupling, the structure is simplified and only passive and semiconductor switching devices are used.

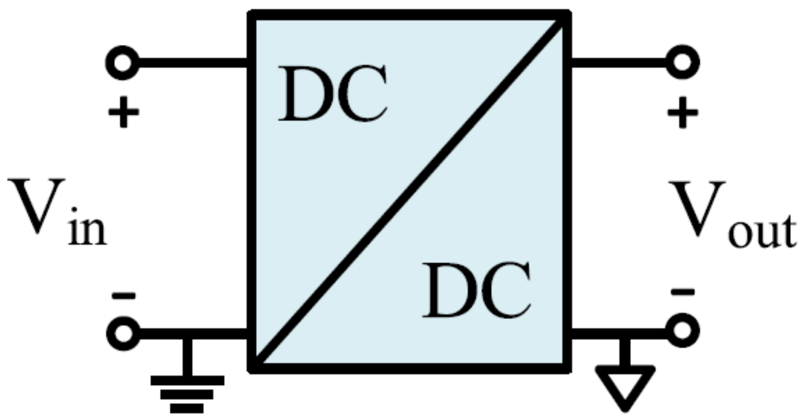

Figure 2.4: Floated-output NI dc/dc converter

2.3 IB dc/dc Converters

For applications demanding a secured power transfer without noise and minimally possible EMI, electrical isolation is provided to make the load side safe from the fluctuations in the source side. Typical example is in grid connected dc/dc converters. Application standard shows that isolated boost dc/dc converters are suitable for many high power applications. For applications with highly sensitive loads, that are susceptible to noise such as loads used in military and medical equipment, safety is a priority and therefore electrical isolation is normally used (V. Garcia, Rico, Sebastih, & Hernando, 1994; Rotman & Ben-Yaakov, 2013; Sun, Ding, Nakaoka, & Takano, 2000). Electrically isolated converters may be constructed as single stage or two stage form. And the isolation is commonly provided through the use of coupling inductor or by using transformers (Chub, Vinnikov, Blaabjerg, & Peng, 2016; Steigerwald, Doncker, & Kheraluwala, 1996; Yao, Ruan, Wang, & Tse, 2011).

In the topologies where coupling inductors are used to provide isolation, the inductor charges and save energy during a cycle and subsequently discharges energy to load in remaining. These topologies employ large switching frequency to minimize the size of the magnetic circuit. The circuit diagram for a single stage coupled-inductor isolated step-up dc/dc converter is shown in Fig. 2.5. Another promising topology of based on coupled inductor method are Flyback converters, which can serve as boost as well as buck. More details on applications that use coupled-inductor dc/dc converters can be found in (B. Axelrod, Berkovich, & Ioinovici, 2003; Liang, Lee, Chen, Chen, & Yang, 2013; W. Song & Lehman, 2007; Yan & Lehman, 2005).

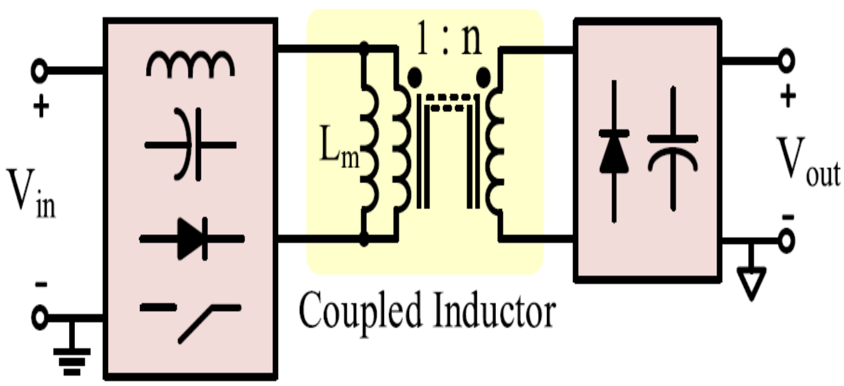

Figure 2.5: Single-stage IBC

The topologies where large frequency transformers are employed to provide isolation, the dc input-voltage first converts to ac-voltage (mostly square-wave), before passing via the transformer. Different switching concepts are used in transformer isolated step-up dc converters depending on the structure. Popular topologies include half-bridge, full-bridge, push-pull and forward converters to mention few (Yao et al., 2011). Additionally, a group of three-stages transformer-isolated dc/dc topologies improved the performance of the classical dc/dc converters by minimizing voltage stresses and current ripples.

Fig. 2.6 illustrated the schematic diagram of a two-level transformer IBC. It is observed auxiliary converter circuit has been added to the primary side so as to normalize the voltage level before supplying to the transformer. The auxiliary converter section may contain an impedance source network or just a single dc/dc converter with its own control and modulation (Chub et al., 2016; Siwakoti, Blaabjerg, Loh, & Town, 2014; Vinnikov & Roasto, 2011). Recently, impedance also called Z-source networks are widely applied in several power transfer applications because of their tremendous success. Z-source networks have a number of advantages including high voltage gain, minimizing voltage stress on the active switches since no additional switch is required when using Z-source network (Siwakoti, Peng, Blaabjerg, Loh, & Town, 2015). For the purpose of comparison, Table 2.1 summarizes the salient features of isolated boost dc converters compared with their Non-isolated counterpart.

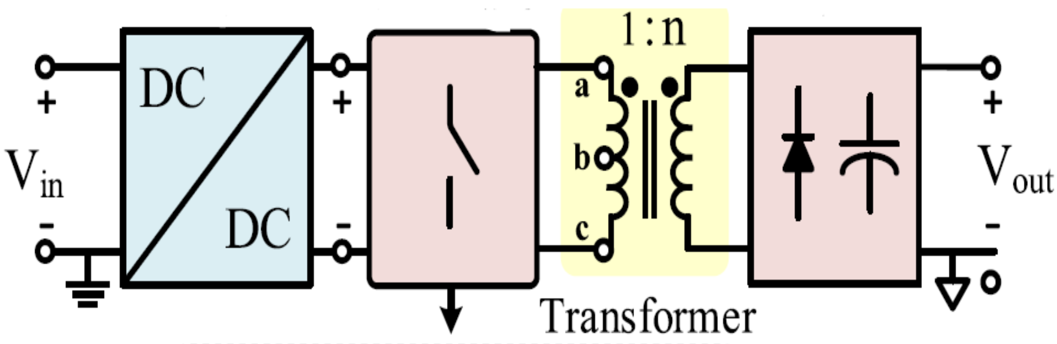

Figure 2.6: Two-stage isolated dc/dc converter

Table 2.1: Important Features of Non-isolated vs Isolated Step-up Converters

Non-isolated step-up	Isolated step-up
❖ Appropriate for conversion from low to medium power stages. ❖ Low weight and cost ❖ Input/output electrical connection	❖ Appropriate for conversion from low to high power stages. ❖ Requires a coupling circuit ❖ Flexible with negative or positive voltages ❖ Suitable for grid connected applications ❖ Less affected by EMI and noise

2.4 CFB dc/dc Converters

Another way of classifying boost converter is by considering nature of input circuitry. Considering this fact, they are categorized into current fed (CFB) and voltage fed boost (VFB) dc converters. In CFB dc converters the input circuit contains an inductive element and can transform the low level voltage at the input to higher level (Nymand & Andersen, 2010)(Lee, Jeong, & Han, 2011). Fig. 2.7 depicted the schematic circuit diagram of the famous full bridge converter, which is an example of current fed dc converters. As shown in the circuit, it contains an output capacitor filter and inductor at the input.

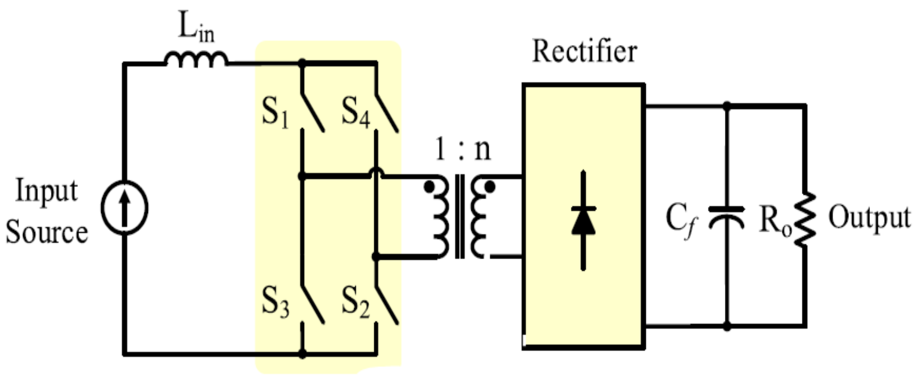

Figure 2.7: CFB full bridge dc converter

Another important example of current fed dc converters are double-inductor double-switch step-up dc converters (Jang & Jovanović, 2004; Lei & Pilawa-Podgurski, 2015). Such converters can be configured as both Non-isolated and isolated structure with a number of rectification modules. Additionally, the performance can be improved by incorporating auxiliary transformer in the input circuitry. Because of the current balance feature of the transformer, when no overlap of switch's on time and therefore no energy will be saved in the inductor. Furthermore, as expressed in (Yan & Lehman, 2005), the weight and size of the converter can be reduced by combining the magnetic devices in a single core, which results in improving power density.

From applicability point of view CFB converters are appropriate in renewable energy applications that have low voltage sources such as fuel cells and photovoltaics. This because the input inductor can guaranty low ripples. This attribute lowers negative impact of current ripples on energy suppliers. Another important feature of CFB dc converts is the fact that they can attain a wide soft-switching and deliver increased efficiency for applications having high input-voltage variations.

2.5 VFB dc/dc Converter

Unlike current-fed, these group contains a capacitor input filter and changes voltage into lesser level at output (Roggia, Schuch, Baggio, Rech, & Pinheiro, 2013; B. Zhao, Yu, Leng, & Chen, 2012). Popular voltage fed bridge converter circuit is depicted in Fig. 2.8. These converter structures contain low pass filter and capacitive filter in their output and input respectively. As discussed in (Yan, Qu, & Lehman, 2003), the magnetic devices can be compacted in single core, minimizing cost and weight. Family of switched-capacitor dc converters, like flying capacitor and multi-level converters are considered to be a form of VFB converters. They generally possess fast response and suits low power applications.

V-source full bridge dc/dc converters suffers from shoot-through condition, due to the switching components at all the legs and the fact that these switches can not switch on simultaneously, but rather the switching process contains time delay in sandwiched between low and high sides of the switches' leg. On the contrary, low and high sides of the switches always contain an overlap, because of the fact that the switches of the I-source full-bridge converter must not switch-off.

Further observation revealed that, absent of inductor at the input of VFB converters leads to high current ripple in the input, yet, since this converter has no right-hand-plane zero, they show faster response compared to CFB converter with input inductor. Nevertheless, Song and Lehman (W. Song & Lehman, 2007) proposed a unique CFB dual bridge dc converter whose voltage transfer-function has no zeroes in the right hand side of complex plane. Which make their voltage conversion ratio to resemble that of VFB dc converter structure presented in (W. Song & Lehman, 2004).

Similarly, the key features of the voltage fed step-up dc/dc converters are compared with the main features of the current fed converter displayed in Table 2.2 the later are intrinsically step- up in nature, and the former are inherently buck in nature.

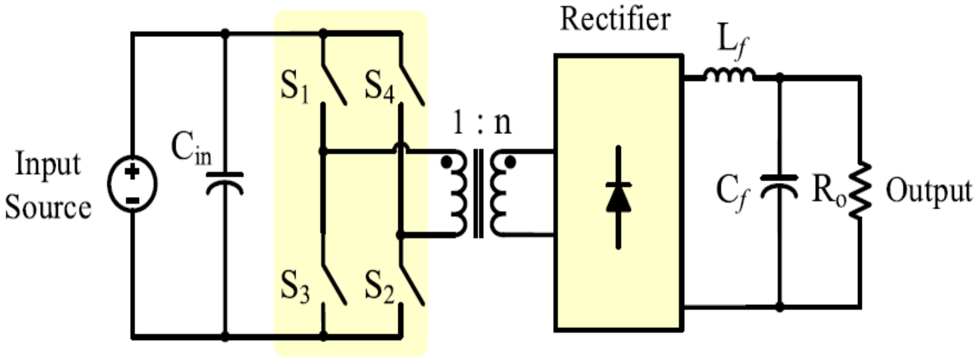

Figure 2.8: VFB full-bridge-converter

Table 2.2: Important Features of CFBC vs VFBC

Current-fed step-up	Voltage-fed step-up
❖ Input current is continuous with little ripples.	❖ Often discontinuous input current with large ripples.
❖ It generally has slow dynamics because of the input inductor.	❖ Generally, has fast dynamics.
	❖ Intrinsic buck characteristics
❖ Intrinsic step-up characteristics	❖ Less affected by EMI and noise

2.6 UB dc/dc Converter

Majority of basic converter circuit are designed for power transfer in only one way, therefore, power should only be supplied from input to output in generation types, from output to input in regeneration (Kobougias & Tatakis, 2010; Matsuo, Harada, & Member, 1976; T. F. Wu & Yu, 1998). In on board applications such as sensor network and other safety equipment, where power flow in one direction, unidirectional converters are used for these purposes. Fig. 2.9 shows a typical structure of unidirectional dc/dc converters, which is built with help of unidirectional components like diode and MOSFET. Fig. 2.10 depicted the classical step-up converter as fundamental UB converter circuit.

Since single quadrant switch is incorporated, in these converters the flow of power is in one direction. There is no return path to conduct current in reverse via diodes. Unidirectional dc converters are excellent choice when power flows in a single direction because of their simple control and drives.

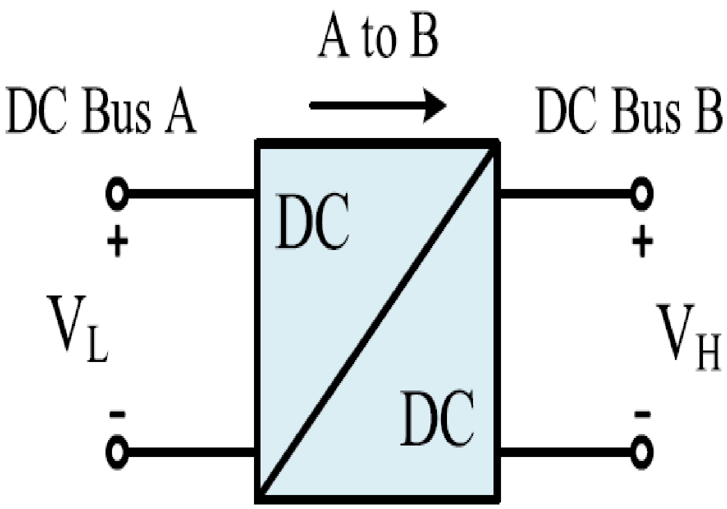

Figure 2.9: General structure unidirectional dc/dc converters

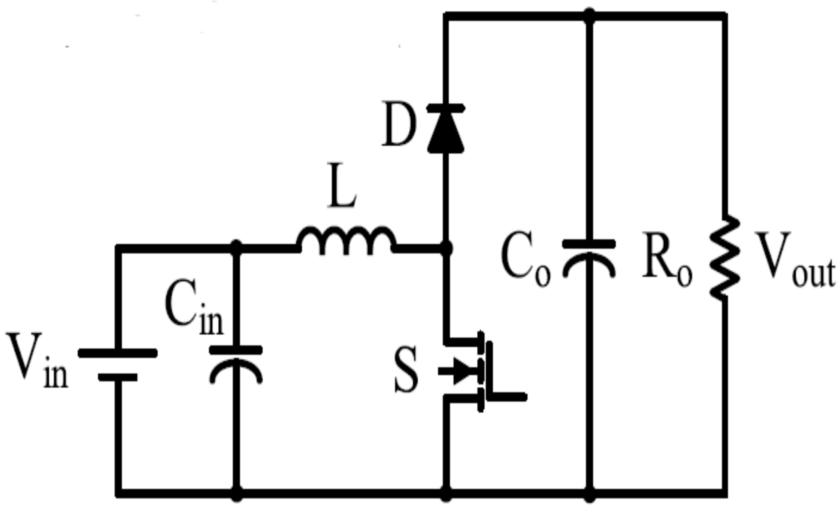

Figure 2.10: Step-up unidirectional dc/dc converter

One useful feature of and design advantage of unidirectional dc converters is diodes have reduced impacts on the power efficiency in contrast to step-down high-power applications. In addition, electrical isolation may be incorporated to improve the performance and safety of these converters or satisfy other needs. Schematic circuit diagram of transformer isolated unidirectional converter depicted in Fig. 2.11. Well known full bridge circuit is a famous example of such converters, especially when for industrial equipment.

These class of converters consists of three stages, dc/ac inverter stage isolation stage and finally ac/dc rectification stage. One key example is having output of full bridge connected to inverter via a capacitor, for ac motor power supply.

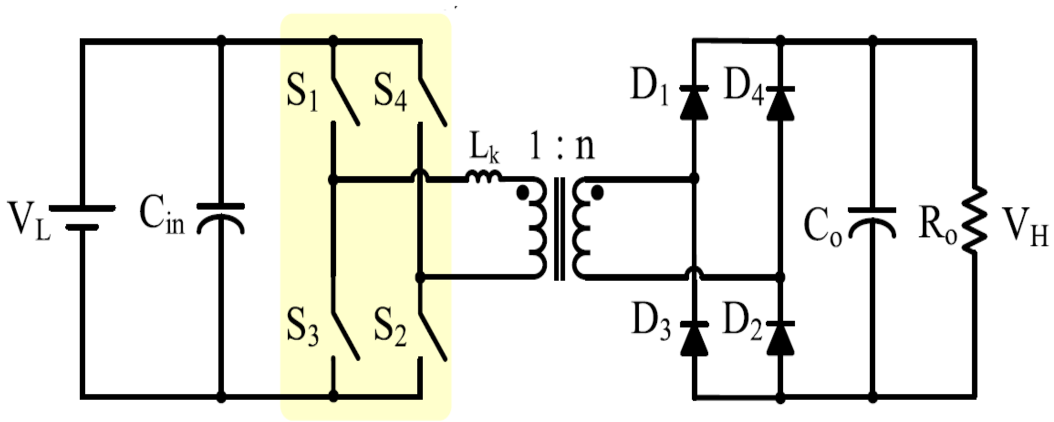

Figure 2.11: Unidirectional isolated dc–dc converter

2.7 BB dc/dc Converters

Given a rapid increase in power equipment that have two way energy transfer ability and storage capability the use of bidirectional dc/dc converters and their design, implementation and manufacturing will dramatically increase. Among its many applications popular ones include hybrid electric vehicle, tramway and train, smart-grid, UPS, vehicle head-lamp, telecommunication applications, dc power-supply and renewable energy to mention few examples (P. Garcia, Fernandez, Garcia, & Jurado, 2010; Li, Hoshina, Satake, & Nogi, 2016). The general structure of bidirectional Non-isolated converter is shown in Fig. 2.12, that can be obtained by using bidirectional semiconductor devices together with double quadrant switches unlike in the unidirectional converter. Fig. 2.13 illustrate a structure of bidirectional boost converter.

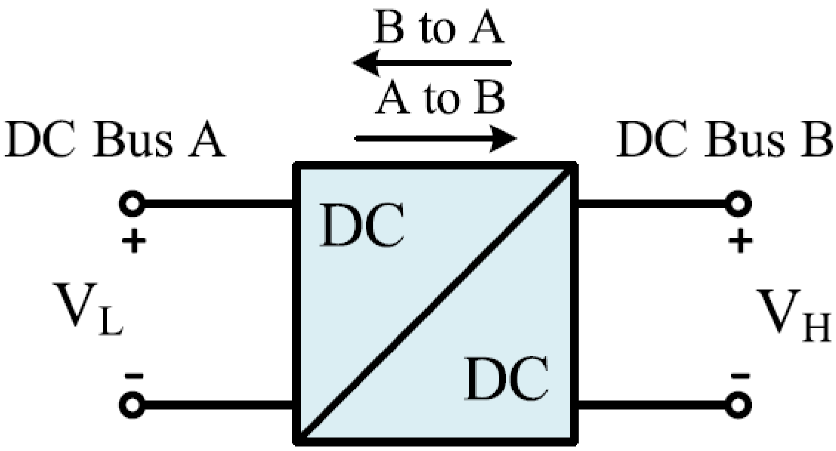

Figure 2.12: General bidirectional converter structure

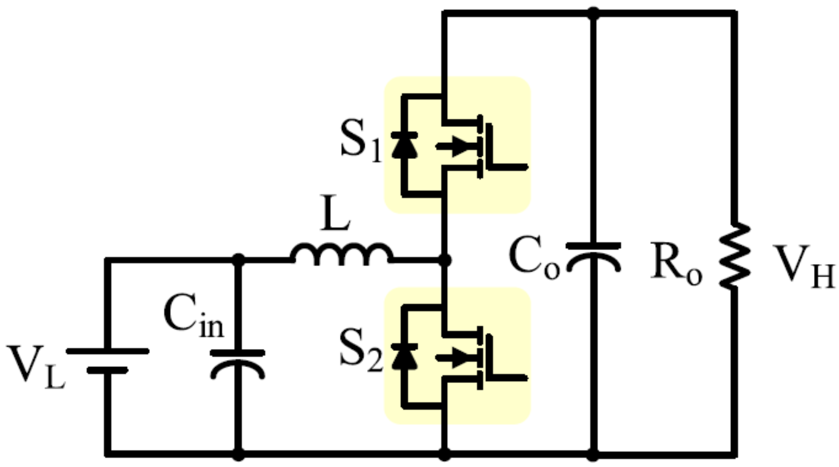

Figure 2.13: Boost type bidirectional converter

In practice, bidirectional converters may be built from combining unidirectional converters. In this case first converter will act as generator to supply energy from the source to the load and the other will serve as a regenerator doing the opposite, i.e to transfer power from load to input. Also, by changing the unidirectional components with bidirectional and bidirectional switch a bidirectional converter structure will be realized. Example of electrically isolated bidirectional dc converter with transformer isolation is shown together with dual-active bridge is shown in Fig. 2.14. Dual active bridge is obtained from unidirectional bridge dc converter circuit. They are highly used in high-power high-voltage applications (Krismer & Kolar, 2012; Naayagi, Forsyth, & Shuttleworth, 2012; Roggia et al., 2013; Thummala, Maksimovic, Zhang, & Andersen, 2016; B. Zhao, Song, Liu, & Sun, 2014).

In the DAB dc/dc structure, power transfer is constrained by varying the phase shifts between waveforms of the voltage in the windings of the transformer. Many researches now concentrate in improving and designing different control strategies for DAB. To wrap-up the discussion of the step-up converters based on power transfer direction a summarized comparison of the main features of bidirectional and unidirectional dc converters a tabulated in Table 2.3.

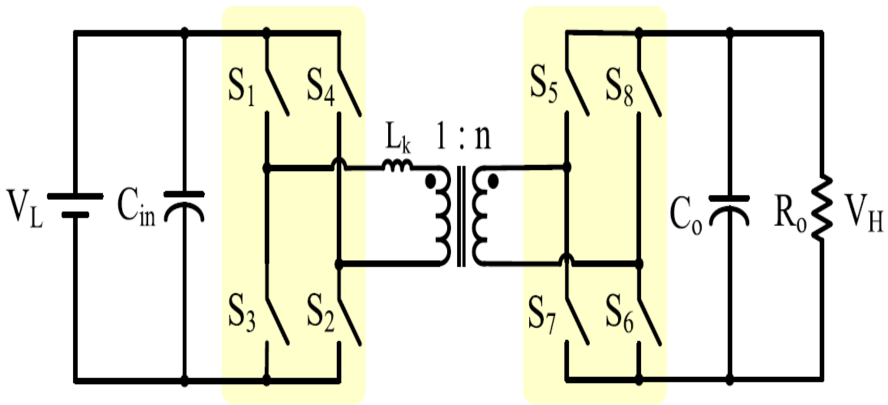

Figure 2.14: DAB isolated bidirectional dc/dc converter

Table 2.3: Important Features of Uni-directional vs Bi-directional Step-up Converters

Uni-directional step-up	Bi-directional step-up
❖ Power flows in a single direction ❖ Lower cost and complexity in comparison to bi-directional ❖ Simple control	❖ Power flows in forward and reverse directions ❖ High cost and complexity compared to unidirectional ❖ Requires a complex FET control and driver unit ❖ Suitable for regenerative applications

2.8 Hard/Soft-Switching dc/dc Converters

The major shortcomings of conventional step-up converters is hard switching which leads to excessive power losses. The power losses happened from the switching procedure where an overlap between the switch-current and switch-voltage at the time of switching transitions generate losses. In theory, these power losses can be eradicated by eliminating the overlap, which may be done by making sure that either the switch's voltage or the switch's current is zero at the time of switch transition. This method is known as "soft-switching techniques".

Moreover, conventional converters because of hard switching suffers from excessive EMI cause by high rate of current and voltage changes during the turn off and on (Chung et al., 1998). Such converters are restricted to low frequency applications because of the increase in losses proportional to increase in frequency. However, high frequency switching is desirable in converters to reduce the overall size of the passive storage elements to realize full miniaturization. Therefore, soft switching converters are proposed to alleviate the challenges of hard switching. They employ resonant circuits with stray capacitance and inductance to obtained zero current switching 'ZCS' and zero voltage switching 'ZVS'. As either current or voltage or both become zero at the time of switch transition, high frequency operation is possible, which means reduction in weight and size will be realized.

Depending on the auxiliary circuit elements used to realized soft-switching, soft-switch converters are categorized resonant containing resonant circuit, snubber containing snubber switches and isolated containing auxiliary circuits.

Resonant converters are preferable in applications requiring high power, since they help in achieving smaller size and weight because of efficiency stability when operating with high frequency. Series, parallel and series/parallel resonant circuits are illustrated in Fig. 2.15 (a)-(c). Similarly, Fig. 2.16 depicted the circuitry of inductor-capacitor-inductor 'LCL", capacitor-inductor-inductor 'CLL' and capacitor-inductor-inductor-capacitor 'CLLC' resonant circuits used in conventional dc converter in order to provide desirable soft-switching (V. Garcia et al., 1994; Han, 2013; Johnson, Witulski, & Erickson, 1988; Senthil Kumar, Siva Ramkumar, Amudha, Balachander, & Emayavaramaban, 2018). However, reliable operation of load-resonant converters depends on resonant-frequency, and operating point conditions, this has limited their applicability for certain conditions.

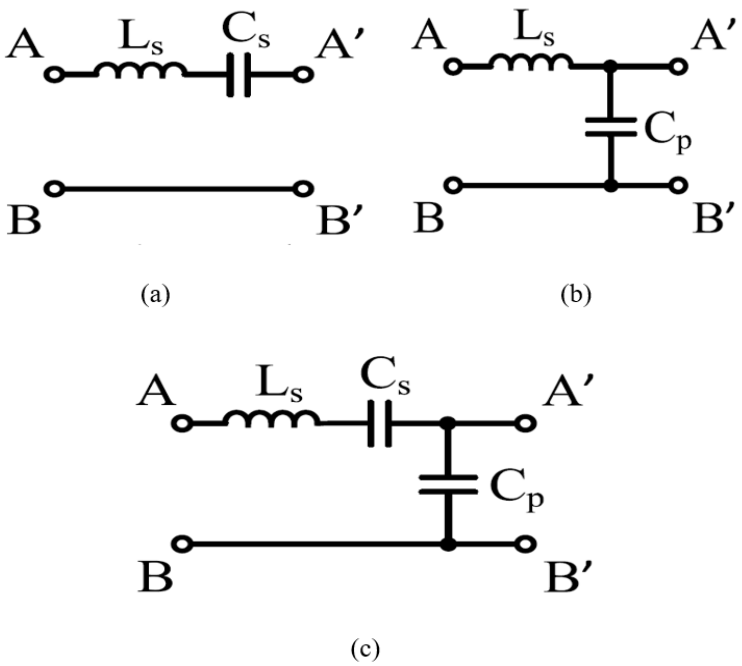

Figure 2.15: (a) Series tank (b) Parallel tank (c) Series-parallel tank

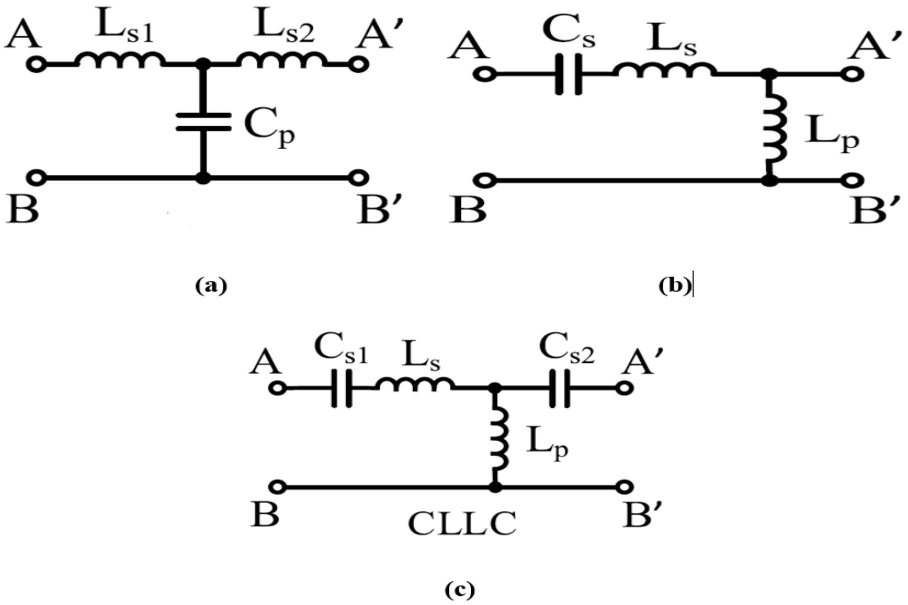

Figure 2.16: (a) LCL (b) CLL (c) CLLC

Alternative set of soft switching converters employ soft switching cells that include active snubbers, ZCT, ZVT, and quasi resonant switch circuits which can be incorporated in conventional dc/dc converters to alleviate the losses due to hard switching (Choi & Cho, 2002; Duarte & Barbi, 1997; C. Wang, 2006). Fig. 2.17 shows example of such switching cells used in dc converters.

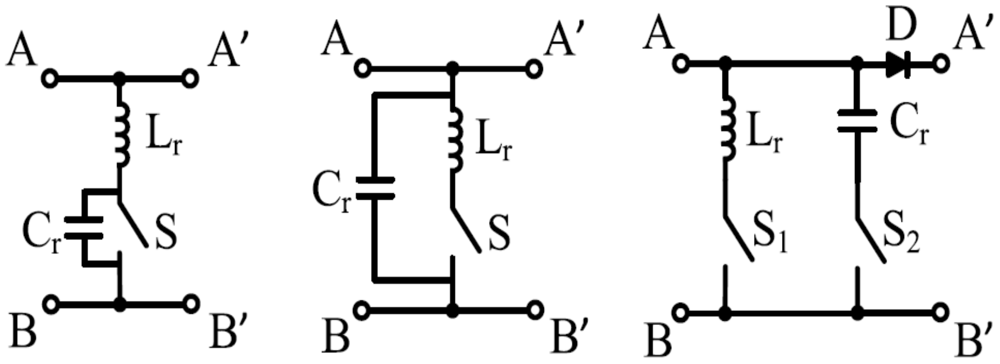

Figure 2.17: Quasi-resonant switching cells

Moreover, the auxiliary network can be made along with isolation inductor or transformer or active networks. For example, Fig. 2.18 and Fig. 2.19 illustrated bridge topologies consisting auxiliary networks to apply soft switching in the primary and secondary sides respectively. These are well investigated topologies with various potential applications. For more detailed on secondary side isolated soft switching converters following references can be referred to (Cho, Rim, & Lee, 1996; Choi, Kim, & Cho, 2002; T. T. Song, Huang, & Ioinovici, 2005), also, for more detailed on primary side isolated soft switching converters following references can be checked (Mao, Abu-qahouq, Luo, Batarseh, & Member, 2004)(Jeon, Canales, Barbosa, & Lee, 2002)(Marx & Schroder, 1996).

In some NIB dc/dc converters hard switching losses are handle through the use of small resonant capacitive element in cascade with either side of the transformer or coupling inductor. These converters also achieved soft switching under all load variations (Forouzesh, Yari, Baghramian, & Hasanpour, 2017; Henrique et al., 2005; Y. Lu, Liu, Hu, Wu, & Xing, 2015). In similar passion, a summary of main characteristics of the SSBC and HSBC presented in Table 2.4.

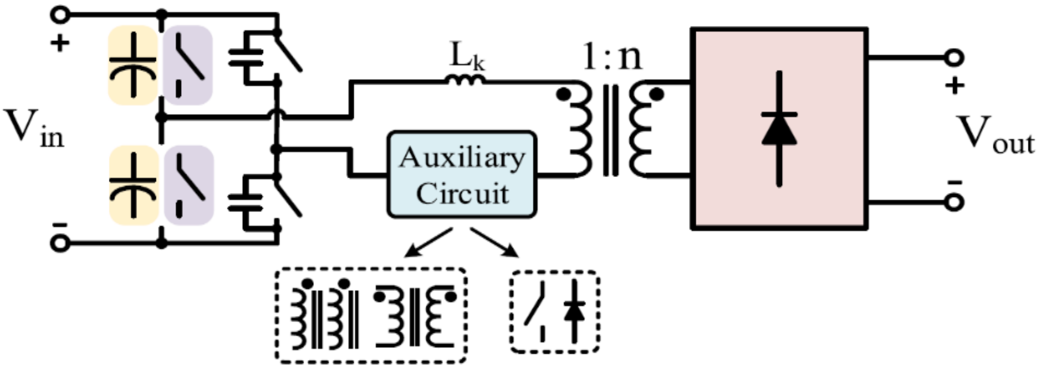

Figure 2.18: Quasi-resonant switching cells

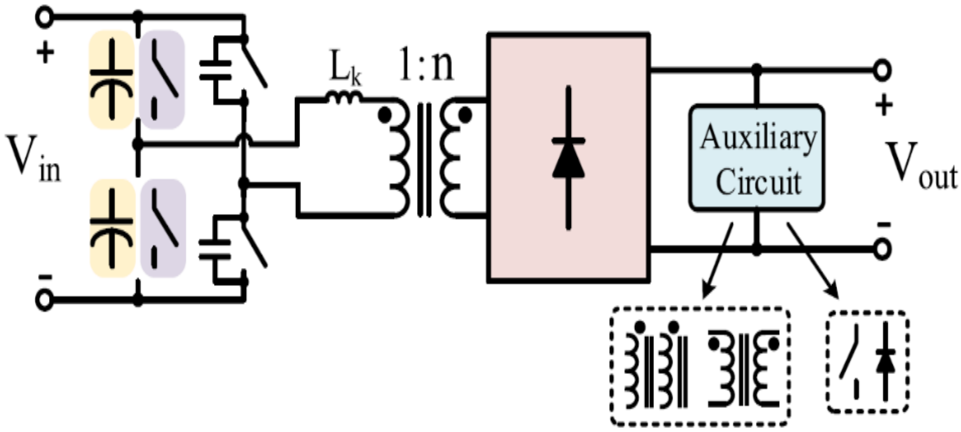

Figure 2.19: Quasi-resonant switching cells

Table 2.4: Important Features of Hard-switching vs Soft-switching Step-up Converters

Hard-Switching Step-up	Soft-Switching Step-up
❖ High switching losses ❖ Limited switching frequency ❖ Reduced efficiency ❖ Low power density ❖ High EMI resulting from high rate of change in voltage and current at the switching transition	❖ ZVS and ZCS with negligible switching losses ❖ High switching frequency ❖ High power density ❖ Increase complexity

CHAPTER 3

CIRCUIT DESIGN, ANALYSIS AND SIMULATION RESULTS

3.1 Introduction

In this chapter, the converter circuits' construction, operation, analysis and simulation result is presented. For this research, step-up converter configuration presented by (Yang, Liang, & Chen, 2009) is studied. Two different step-up converters are chose. The steady analysis is carried out for the converters while operating in both continuous conduction and discontinuous conduction modes. For the purpose of comparison, the analysed converters are compared with a classical boost converter to depict the superiority of the former. A simulation is conducted using PSCAD and the result is reported at the end of the chapter.

Following assumptions are made for the steady-state analysis:

1) The converter components are ideal;

2) Active switches' ON resistance RDS_{ON}, Inductors and capacitors $ESRs$ and diodes' forward voltage drop are neglected

3) The voltage across the capacitors is assumed to remain constant.

3.2 Operating Principle and Steady-state Analysis of Circuit I

The first converter circuit configuration is shown in Fig. 3.1. This circuit is formed by using two identical inductors L_1 and L_2 (having the same inductance), two switches S_1 and S_2; controlled by the same signal simultaneously, a single output capacitor C_o, single output diode D_o and a load resistor R. As shown in the waveform Fig. 3.2, the converter operates in both CCM and DCM. Detailed analysis in CCM and DCM is described in subsection 3.2.1 and subsection 3.2.2 respectively.

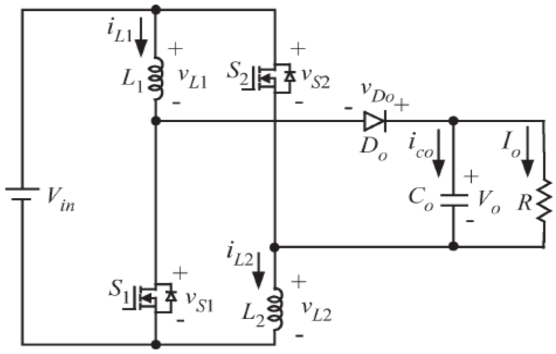

Figure 3.1: Converter circuit I

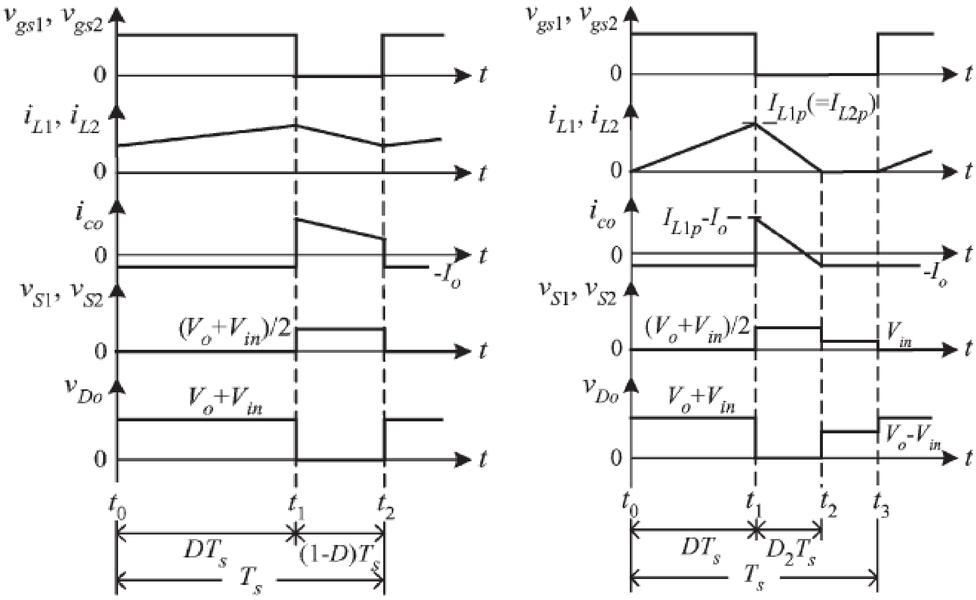

(a) (b)

Figure 3.2: Converter circuit I operating waveforms. (a) CCM (b) DCM

3.2.1 Circuit I continuous conduction mode operation

The CCM operating mode, as illustrated in Fig. 3.2 (a), is comprised of two modes, which are explained below.

a) Mode I: $t \in [t_0, t_1]$

For the first time interval, with equivalent circuit depicted in Fig. 3.3. In this time interval, both switches S_1 and S_2 are on. The dc source charges the identical inductors L_2 and L_1 are parallel to one another, in addition, capacitor C_o supplies stored-energy towards load. Applying KVL to circuit in Fig. 3.3, voltage across inductors L_1 and L_2 is obtained as

$$-V_{in} + v_{L1} = 0$$
$$-V_{in} + v_{L2} = 0$$
$$v_{L1} = v_{L2} = V_{in} \tag{3.1}$$

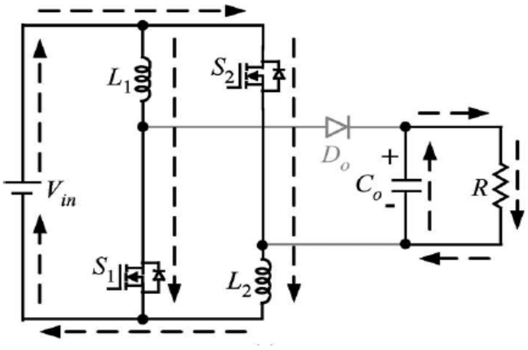

Figure 3.3: Converter I equivalent circuit when switches are on

b) Mode II: $t \in [t_1, t_2]$

For the second time interval, with equivalent circuit depicted in Fig. 3.4. Within the time interval, both the switch S_1 and switch S_2 become off. As seen in Fig. 3.4, the inductors L_2, L_1 are cascaded with V_{in} and therefore transfer energy to the output capacitor C_o and the load R.

Similarly, by applying KVL in the equivalent circuit, the inductor voltages can be obtained as

$$-V_{in} + v_{L1} + v_{L2} + V_o = 0$$
$$v_{L1} + v_{L2} = V_{in} - V_o$$
$$v_{L1} = v_{L2} \text{ (identical inductors)}$$

And therefore,

$$v_{L1} = v_{L2} = \frac{V_{in} - V_o}{2} \tag{3.2}$$

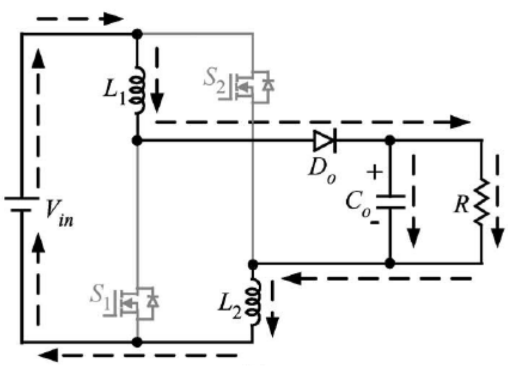

Figure 3.4: Converter I equivalent circuit when switches are off

Now, to obtained the voltage gain during the CCM operation mode, using volt-second balance property of the inductors, we get

$$\int_0^T v_L dt = 0 \tag{3.3}$$

Substituting for v_L in (3.3) from (3.1) and (3.2)

$$\int_0^{DT_s} V_{in} dt + \int_{DT_s}^{T_s} \left(\frac{V_{in}-V_o}{2}\right) dt = 0 \tag{3.4}$$

$$V_{in}(DT_s - 0) + {}^1/_2\,(V_{in} - V_o)(T_s - DT_s) = 0$$

$$T_s(2V_{in}D + V_{in} - V_o - V_{in}D + V_oD) = 0$$

$$V_{in}(1 + D) - V_o(1 - D) = 0$$

And hence, the voltage gain in CCM for converter I G_{CCMI} is

$$G_{CCMI} = \frac{V_o}{V_{in}} = \frac{(1+D)}{(1-D)} \tag{3.5}$$

The voltage stress across the semiconductor devices can be obtained from the CCM waveform Fig. 3.2 (a) as

$$V_{S1} = V_{S2} = \frac{V_o+V_{in}}{2} \tag{3.6}$$

$$V_{Do} = V_o + V_{in} \tag{3.7}$$

3.2.2 Circuit I discontinuous conduction mode operation

The DCM operating mode is described by the waveform shown in Fig. 3.2 (b). This can be explained in three different modes.

a) Mode I: $t \in [t_0, t_1]$

For this mode the converter operation is similar to its operation in CCM mode I. Therefore, the maximum value inductor current is

$$I_{L1p} = I_{L2p} = \frac{1}{L}\int_0^{DT_s} V_{in} dt \tag{3.8}$$

$$= \frac{V_{in}}{L}(DT_s - 0)$$

And therefore,

$$I_{L1p} = I_{L2p} = \frac{V_{in}}{L} DT_s \tag{3.9}$$

L represents the inductance of the two inductors.

b) Mode II: $t \in [t_1, t_2]$

During the period between times t_1 and t_2 the switches are off as shown in Fig. 3.4. As shown, inductors are in series with the dc voltage source V_{in} and transmit energy to C_o and R. At the time t_2, the currents of the inductors become zero. For this time interval, the peak currents of the two inductors are given by

$$I_{L1p} = I_{L2p} = \frac{(V_o - V_{in})}{2L} D_2 T_s \tag{3.10}$$

c) Mode III: $t \in [t_2, t_3]$

In the time interval between t_2 and t_3 the switches remained in the off state, as shown in the equivalent circuit of Fig. 3.5. At this moment there is no energy in the inductors L_1 and L_2. Subsequently, energy saved in C_o is transferred R. Using equations (3.9) and (3.10), D_2 is obtained as

$$\frac{V_{in}}{L} D T_s = \frac{(V_o - V_{in})}{2L} D_2 T_s$$

$$D_2 = \frac{2 V_{in} D}{(V_o - V_{in})} \tag{3.11}$$

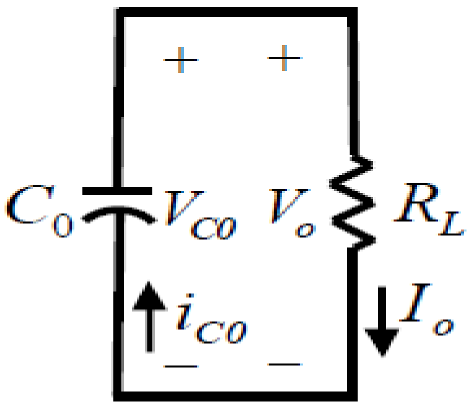

Figure 3.5: DCM equivalent circuit of converter I with switches off

From the waveform in Fig. 3.2 (b), for each period the average capacitor current I_{co} is obtained as

$$I_{co} = \frac{\frac{1}{2} D_2 T_s I_{L1p} - I_o T_s}{T_s}$$

Further simplification gives

$$I_{co} = \frac{1}{2} D_2 I_{L1p} - I_o \tag{3.12}$$

Were I_o is the output current and is given as

$$I_o = \frac{V_o}{R} \tag{3.13}$$

Substituting for I_{L1p}, D_2 and I_o from (3.9), (3.11) and (3.13) in to (3.12)

$$I_{co} = \frac{1}{2}\left(\frac{2V_{in}D}{(V_o - V_{in})}\right)\left(\frac{V_{in}}{L}DT_s\right) - \frac{V_o}{R}$$

And this is simplified to

$$I_{co} = \frac{V_{in}^2 D^2 T_s}{L(V_o - V_{in})} - \frac{V_o}{R} \tag{3.14}$$

Under steady state, I_{co} is zero, therefore (3.14) becomes

$$\frac{V_{in}^2 D^2 T_s}{L(V_o - V_{in})} = \frac{V_o}{R}$$

$$\frac{V_{in}^2 D^2}{V_o(V_o - V_{in})} = \frac{L}{T_s R} \tag{3.15}$$

Denoting the switching frequency as $f_s = \frac{1}{T_s}$, and substituting into equation (3.15), we have

$$\frac{V_{in}^2 D^2}{V_o(V_o - V_{in})} = \frac{Lf_s}{R} \tag{3.16}$$

The inductor time-constant can, therefore, be defined as

$$\tau_L = \frac{Lf_s}{R} \tag{3.17}$$

By using (3.17) in to (3.16)

$$\frac{V_{in}^2 D^2}{V_o(V_o - V_{in})} = \tau_L$$

$$\frac{V_{in}^2}{V_o(V_o - V_{in})} = \frac{\tau_L}{D^2}$$

$$\frac{V_o^2 - V_o V_{in}}{V_{in}^2} = \frac{D^2}{\tau_L}$$

And can be express as a second-order polynomial

$$\left(\frac{V_o}{V_{in}}\right)^2 - \left(\frac{V_o}{V_{in}}\right) - \left(\frac{D^2}{\tau_L}\right) = 0 \tag{3.18}$$

Let $\frac{V_o}{V_{in}} = x$

$$x^2 - x - \left(\frac{D^2}{\tau_L}\right) = 0 \tag{3.19}$$

Solving (3.19) using the quadratic formula

$$x = \frac{-b \pm \sqrt{b^2 - 4ac}}{2a} \tag{3.20}$$

The DCM voltage gain G_{DCMI} can be express as

$$G_{DCMI} = \frac{V_o}{V_{in}} = \frac{1}{2} + \sqrt{\frac{1}{4} + \frac{D^2}{\tau_L}} \tag{3.21}$$

3.2.3 Circuit I boundary conduction mode operation

The converter is said to be operating in so-called "boundary conduction mode (BCM)" when CCM gain is same as DCM gain. By equating (3.5) to (3.21), normalized time-constant for the BCM is

$$\frac{(1+D)}{(1-D)} = \frac{1}{2} + \sqrt{\frac{1}{4} + \frac{D^2}{\tau_{LB}}}$$

$$\frac{(1+D)}{(1-D)} - \frac{1}{2} = \sqrt{\frac{1}{4} + \frac{D^2}{\tau_{LB}}}$$

$$\frac{(1+D)^2}{(1-D)^2} - \frac{(1+D)}{(1-D)} + \frac{1}{4} = \frac{1}{4} + \frac{D^2}{\tau_{LB}}$$

$$\frac{(1+D)^2}{(1-D)^2} - \frac{(1+D)}{(1-D)} = \frac{D^2}{\tau_{LB}}$$

$$\tau_{LB} = \frac{D^2(1-D)^2}{2(D+D^2)}$$

And therefore τ_{LB} is given by

$$\tau_{LB} = \frac{D(1-D)^2}{2(1+D)} \tag{3.21}$$

Fig. 3.6 shows the curve of τ_{LB}, is seen from the figure when $\tau_L < \tau_{LB}$ the converter operates in DCM, and it operates in CCM when $\tau_L > \tau_{LB}$.

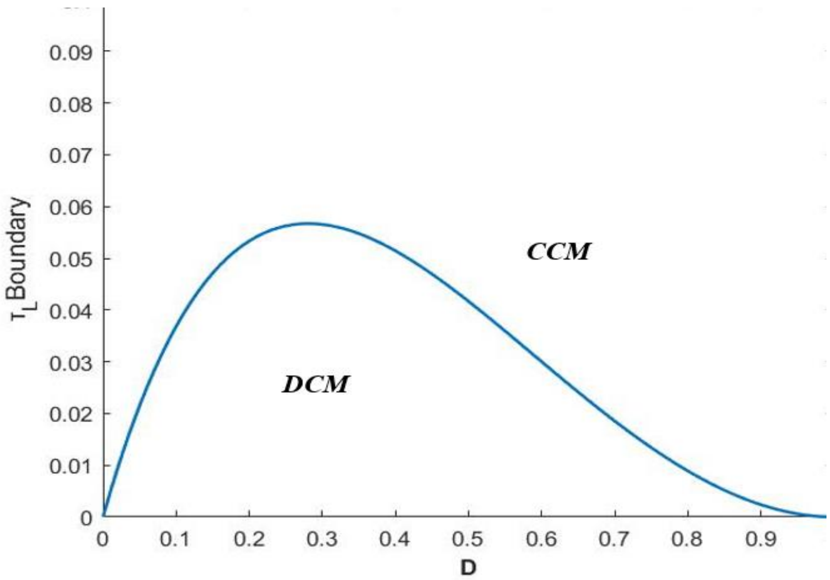

Figure 3.6: Circuit I boundary operation condition

3.3 Operating Principle and Steady-state Analysis of Circuit II

The second converter circuit configuration is shown in Fig. 3.7. This circuit is formed by adding voltage lift circuits to the converter circuit I shown in Fig.3.1. Therefore, two identical inductors are used, along with two switches S_1 and S_2; being controlled by the same signal simultaneously, a single output capacitor C_o, single output diode D_o and a load resistor R. Each voltage lift circuit comprises a single capacitor and inductor. As shown in the waveform Fig. 3.8, the converter operates in both CCM and DCM. The CCM and DCM analysis is presented in subsection 3.3.1 and 3.3.2 respectively.

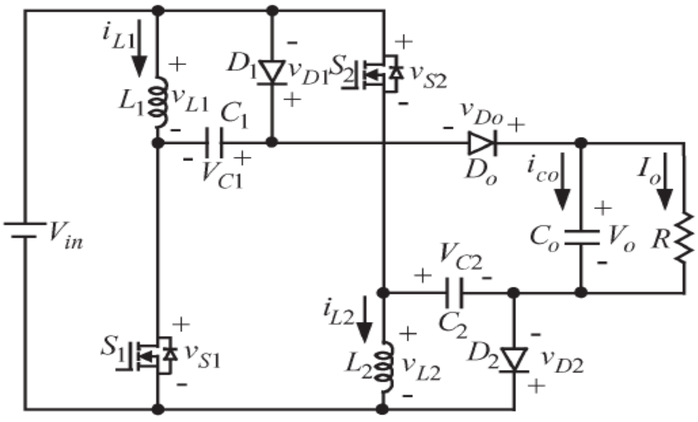

Figure 3.7: Converter circuit II

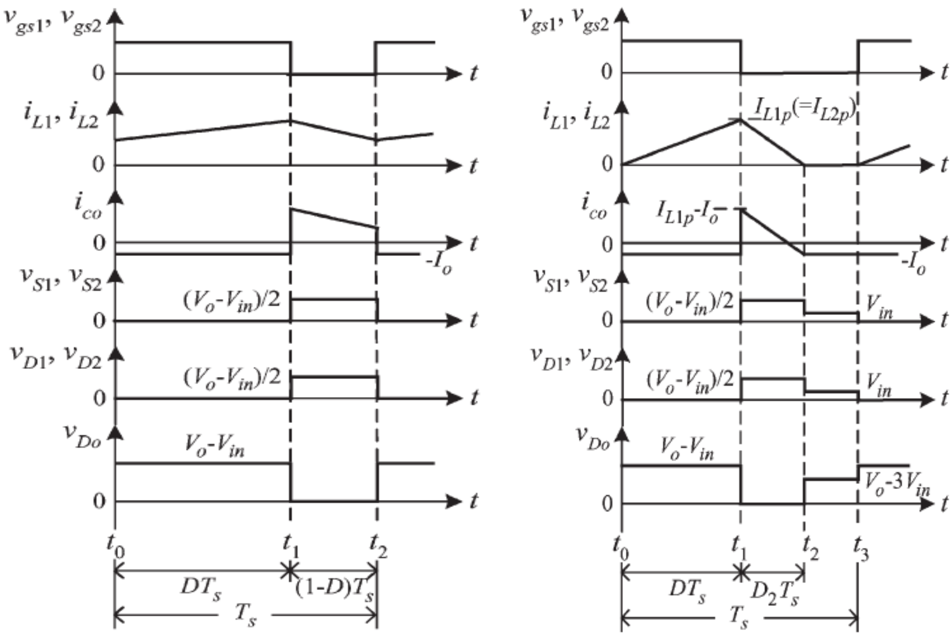

(a) (b)

Figure 3.8: Converter circuit II operating waveforms. (a) CCM (b) DCM

3.3.1 Circuit II continuous conduction mode operation

The CCM operating mode, as depicted in Fig. 3.8 (a), is comprised of two modes, which are referred to as mode I and mode II.

a) Mode I: $t \in [t_0, t_1]$

The equivalent circuit representing mode I is shown in Fig. 3.9. Within this period the switches are on. The dc source charges the identical inductors while the capacitor C_o supply its saved energy R_L. Applying KVL to circuit in Fig. 3.9, the voltage across the inductors L_1 and L_2 and capacitors C_1 and C_2 is obtained as

$$v_{L1} = v_{L2} = V_{C1} = V_{C2} = V_{in} \tag{3.22}$$

b) Mode II: $t \in [t_1, t_2]$

Fig. 3.10 illustrate resultant circuit for this mode. Within this period, both switches are off. As seen in Fig. 3.10, the two inductors and the capacitors are in cascade with the V_{in} and therefore energy is to the output-capacitor C_o and the load R.

Similarly, by applying KVL in the equivalent circuit, the inductor voltages can be obtained as

$$-V_{in} + v_{L1} - V_{C1} + V_o - V_{C2} + v_{L2} = 0$$

$v_{L1} = v_{L2}$ (identical inductors)

$$v_{L1} = v_{L2} = \frac{V_{in} + V_{C1} + V_{C2} - V_o}{2}$$

$$V_{C1} = V_{C2} = V_{in}$$

Thus,

$$v_{L1} = v_{L2} = \frac{3V_{in} - V_o}{2} \tag{3.23}$$

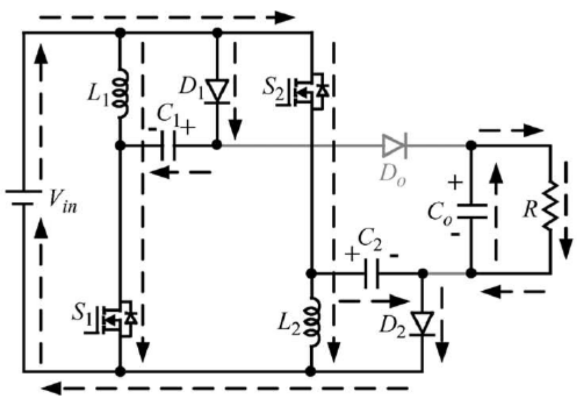

Figure 3.9: Equivalent circuit of converter II with switches on

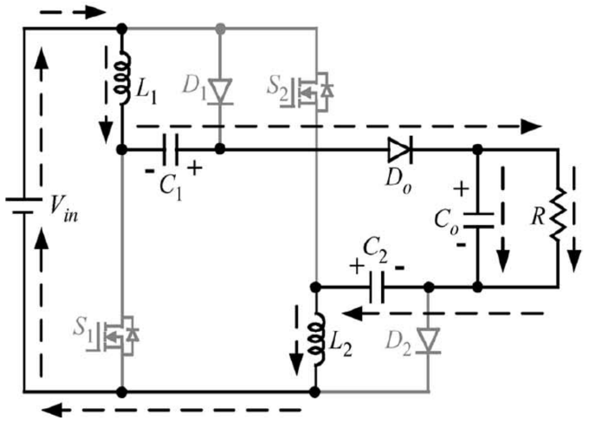

Figure 3.10: Equivalent circuit of converter II with switches off

Furthermore, to determine the voltage gain for the converter circuit II under CCM operation mode, volt-second balance property of the inductors is used as follows:

$$\int_0^T v_L dt = 0$$

Substituting for v_L using (3.22) and (3.23)

$$\int_0^{DT_s} V_{in} dt + \int_{DT_s}^{T_s} \left(\frac{3V_{in} - V_o}{2}\right) dt = 0 \tag{3.24}$$

$$V_{in}(DT_s - 0) + {}^1\!/_2\,(3V_{in} - V_o)(T_s - DT_s) = 0$$

$$T_s(2V_{in}D + 3V_{in} - 3V_{in}D - V_o + V_oD) = 0$$

$$V_{in}(2D + 3 - 3D) - V_o(1 - D) = 0$$

$$V_{in}(3 - D) = V_o(1 - D)$$

And hence, the voltage gain in CCM for converter II G_{CCMII} is

$$G_{CCMII} = \frac{V_o}{V_{in}} = \frac{(3-D)}{(1-D)} \tag{3.25}$$

The voltage stress across the semiconductor devices can be obtained from the CCM waveform Fig. 3.8 (a) as

$$V_{S1} = V_{S2} = V_{D1} = V_{D2} = \frac{V_o - V_{in}}{2} \tag{3.26}$$

and,

$$V_{Do} = V_o - V_{in} \tag{3.27}$$

3.3.2 Circuit II discontinues conduction mode operation

This section describe the DCM operating mode by the waveform shown in Fig. 3.8 (b). Moreover, it can be explained in three different modes.

a) Mode I: $t \in [t_0, t_1]$

The converter operation is in this time period is similar to its operation in CCM mode I. Therefore, the maximum inductor $I_{L1p} = I_{L2p}$ and is given by

$$I_{L1p} = I_{L2p} = \frac{1}{L}\int_0^{DT_s} V_{in} dt \tag{3.28}$$

$$= \frac{V_{in}}{L}(DT_s - 0)$$

And therefore,

$$I_{L1p} = I_{L2p} = \frac{V_{in}}{L} DT_s \tag{3.29}$$

b) Mode II: $t \in [t_1, t_2]$

During the period between times t_1 and t_2 the switches are off as shown in Fig. 3.10. As shown, inductors and capacitors are in series with the dc voltage source V_{in} and transmit energy to C_o and R. At the time $t = t_2$, the inductor currents i_{L1} and i_{L2} decreases to zero. The peak currents can also be expressed as

$$I_{L1p} = I_{L2p} = \frac{V_o - V_{in} - V_{C1} - V_{C2}}{2L} D_2 T_s$$

$$= \frac{V_o - 3V_{in}}{2L} D_2 T_s \tag{3.30}$$

c) Mode III: $t \in [t_2, t_3]$

In the time interval between t_2 and t_3 the switches remained in the off state, as shown in the equivalent circuit of Fig. 3.11. At this moment there is no energy in the inductors L_1 and L_2. Afterwards, energy saved in C_o is transferred R. Using equations (3.29) and (3.30), D_2 is obtained as

$$\frac{V_{in}}{L} DT_s = \frac{V_o - 3V_{in}}{2L} D_2 T_s$$

$$D_2 = \frac{2V_{in}D}{(V_o - 3V_{in})} \tag{3.31}$$

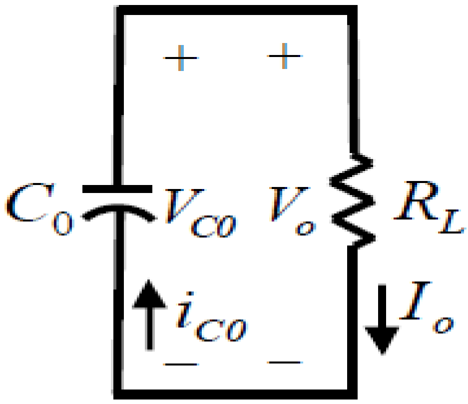

Figure 3.11: DCM equivalent circuit of converter II with switches off

From the waveform in Fig. 3.8 (b), over each period of the switching cycle, the average capacitor current I_{co} is

$$I_{co} = \frac{\frac{1}{2}D_2 T_s I_{L1p} - I_o T_s}{T_s}$$

Further simplification gives

$$I_{co} = \frac{1}{2} D_2 I_{L1p} - I_o \tag{3.32}$$

Were I_o is the output current and is given as

$$I_o = \frac{V_o}{R} \tag{3.33}$$

Substituting for I_{L1p}, D_2 and I_o from (3.29), (3.31) and (3.33) in to (3.32)

$$I_{co} = \frac{1}{2}\left(\frac{2V_{in}D}{(V_o - 3V_{in})}\right)\left(\frac{V_{in}}{L} DT_s\right) - \frac{V_o}{R}$$

And this is simplified to

$$I_{co} = \frac{V_{in}^2 D^2 T_s}{L(V_o - 3V_{in})} - \frac{V_o}{R} \tag{3.34}$$

under steady state, I_{co} is zero, hence (3.34) becomes

$$\frac{V_{in}^2 D^2 T_s}{L(V_o - 3V_{in})} = \frac{V_o}{R}$$

$$\frac{V_{in}^2 D^2}{V_o(V_o - 3V_{in})} = \frac{L}{T_s R} \tag{3.35}$$

Substituting for $f_s = \frac{1}{T_s}$ into equation (3.35), we have

$$\frac{V_{in}^2 D^2}{V_o(V_o - 3V_{in})} = \frac{L f_s}{R} \tag{3.36}$$

The inductor time-constant can, therefore, be expressed as

$$\tau_L = \frac{Lf_s}{R} \tag{3.37}$$

Substituting for τ_L from (3.37) in to (3.36)

$$\frac{V_{in}^2 D^2}{V_o(V_o - 3V_{in})} = \tau_L$$

$$\frac{V_o^2 - 3V_oV_{in}}{V_{in}^2} = \frac{D^2}{\tau_L}$$

$$\left(\frac{V_o}{V_{in}}\right)^2 - 3\left(\frac{V_o}{V_{in}}\right) - \left(\frac{D^2}{\tau_L}\right) = 0 \tag{3.38}$$

By letting $\frac{V_o}{V_{in}} = x$

$$x^2 - x - \left(\frac{D^2}{\tau_L}\right) = 0 \tag{3.39}$$

Solving (3.39) using the quadratic formula

The DCM voltage gain G_{DCMII} can be express as

$$G_{DCMII} = \frac{V_o}{V_{in}} = \frac{3}{2} + \sqrt{\frac{9}{4} + \frac{D^2}{\tau_L}} \tag{3.40}$$

3.3.3 Circuit II boundary conduction mode operation

In a similar way, the converter boundary operating condition is obtained by equating the CCM gains to DCM gain. Equating (3.25) to (3.40), the normalized time-constant in BCM expressed as

$$\frac{(3-D)}{(1-D)} = \frac{3}{2} + \sqrt{\frac{9}{4} + \frac{D^2}{\tau_{LB}}}$$

$$\frac{(3-D)}{(1-D)} - \frac{3}{2} = \sqrt{\frac{9}{4} + \frac{D^2}{\tau_{LB}}}$$

$$\left(\frac{(3-D)}{(1-D)}\right)^2 - 3\frac{(3-D)}{(1-D)} + \frac{9}{4} = \frac{9}{4} + \frac{D^2}{\tau_{LB}}$$

$$\frac{(3-D)^2}{(1-D)^2} - 3\frac{(3-D)}{(1-D)} = \frac{D^2}{\tau_{LB}}$$

And therefore τ_{LB} is given by

$$\tau_{LB} = \frac{D(1-D)^2}{2(3-D)} \tag{3.41}$$

Fig. 3.12 shows the curve of τ_{LB}. It can be seen from the figure that when $\tau_L < \tau_{LB}$ the converter operates in DCM, and it operates in CCM when $\tau_L > \tau_{LB}$.

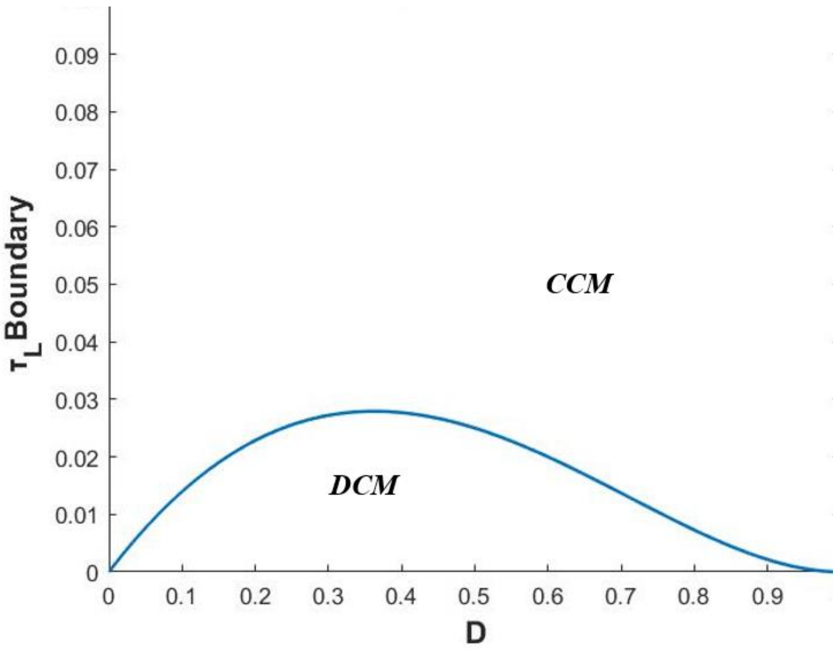

Figure 3.12: Circuit II boundary operation condition

3.4 Performance Comparison

In order to make a performance comparison, the two converter circuits analysed here, are compared with traditional boost converter. The voltage gains and voltage stress are used as presented in Table 3.1. It can be clearly seen that the two converter circuits outperformed the classical boost converter by increasing the voltage gain while at the same time decreasing the voltage stress across the active switches. Figure 3.13 shows the voltage gain curves of the two converters in comparison with the classical one.

Table 3.1: Performance comparison based on voltage gain and voltage stress

	Voltage gain (G_{CCM})	**Voltage stress**
Classical boost converter	$\frac{1}{(1-D)}$	V_o
New boost converter I	$\frac{(1+D)}{(1-D)}$	$\frac{V_o + V_{in}}{2}$
New boost converter II	$\frac{(3-D)}{(1-D)}$	$\frac{V_o - V_{in}}{2}$

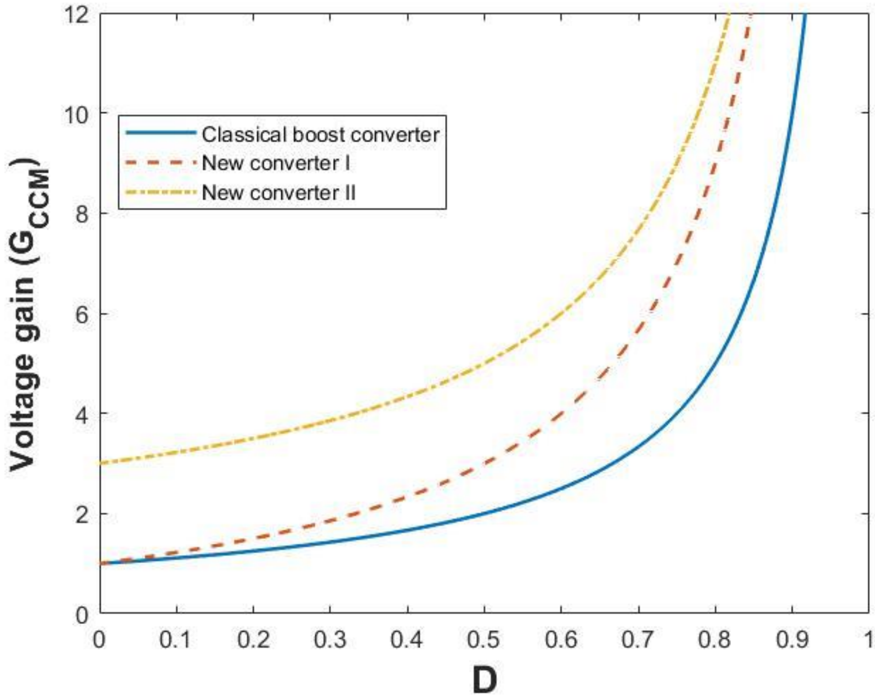

Fig. 3.13: CCM voltage gain vs duty ration

3.5 Simulation Results

The two circuits are analyzed are simulated to demonstrate their practical applicability and validate the theoretical results. Software-based simulations are commonly used after the design phase to show the system's operation over time. Power System Computer-Aided Design (PSCAD) has become a popular power system and power electronics software since its invention, and therefore, PSCAD / EMTDC-V4.2 is used in this thesis for the simulation.

3.5.1 Converter circuit I simulation result

For the simulation of the converter I have shown in Fig. 3.1, the converter components have been selected to be $V_{in} = 12\,V, f_S = 100\,kHz, C_o = 68\,\mu F, D = 0.6\ and\ R = 90\,\Omega$, for the input voltage, switching frequency, the capacitance of the output capacitor, duty ratio and load resistor. To find the suitable value for the inductance, first, the boundary normalized inductor time constant is evaluated using Eq. (3.21) as

$$\tau_{LB} = \frac{D(1-D)^2}{2(1+D)}$$

$$\tau_{LB} = \frac{0.6(1-0.6)^2}{2(1+0.6)} = 0.03$$

And therefore, the inductor time constant

$$\tau_L = \frac{Lf_s}{R} > 0.03 \text{ for CCM}$$

$$\tau_L = \frac{Lf_s}{R} < 0.03 \text{ for DCM}$$

Based on the selected values of the switching frequency f_s and load resistance R the inductor value should be

$$L < \frac{0.03R}{f_s} < 27\ \mu H \quad \text{for DCM} \tag{3.42}$$

$$L > 27\ \mu H \quad \text{for CCM} \tag{3.43}$$

For clarity the selected parameters are presented in Table 3.2

Table 3.2: Selected parameters for simulation

Parameter	**Value**
V_{in}	$12\ V$
f_S	$100\ kHz$
C_o	$68\ \mu F$
D	0.6
$L_1 = L_2$ (CCM)	$100\ \mu H$
$L_1 = L_2$ (DCM)	$20\ \mu H$
R	$90\ \Omega$

Fig. 3.14 shows the graph of the input voltage, output voltage, input current and output current for the converter circuit I. It can be observed that for the input voltage equal to 12 V the steady-state output voltage is found to be equal to 48 V, which satisfies the CCM voltage gain relationship given by equation (3.5). Similarly, the steady-state output current is approximately equal to 0.533 A which is equal to ${}^{V_o}/_{R}$.

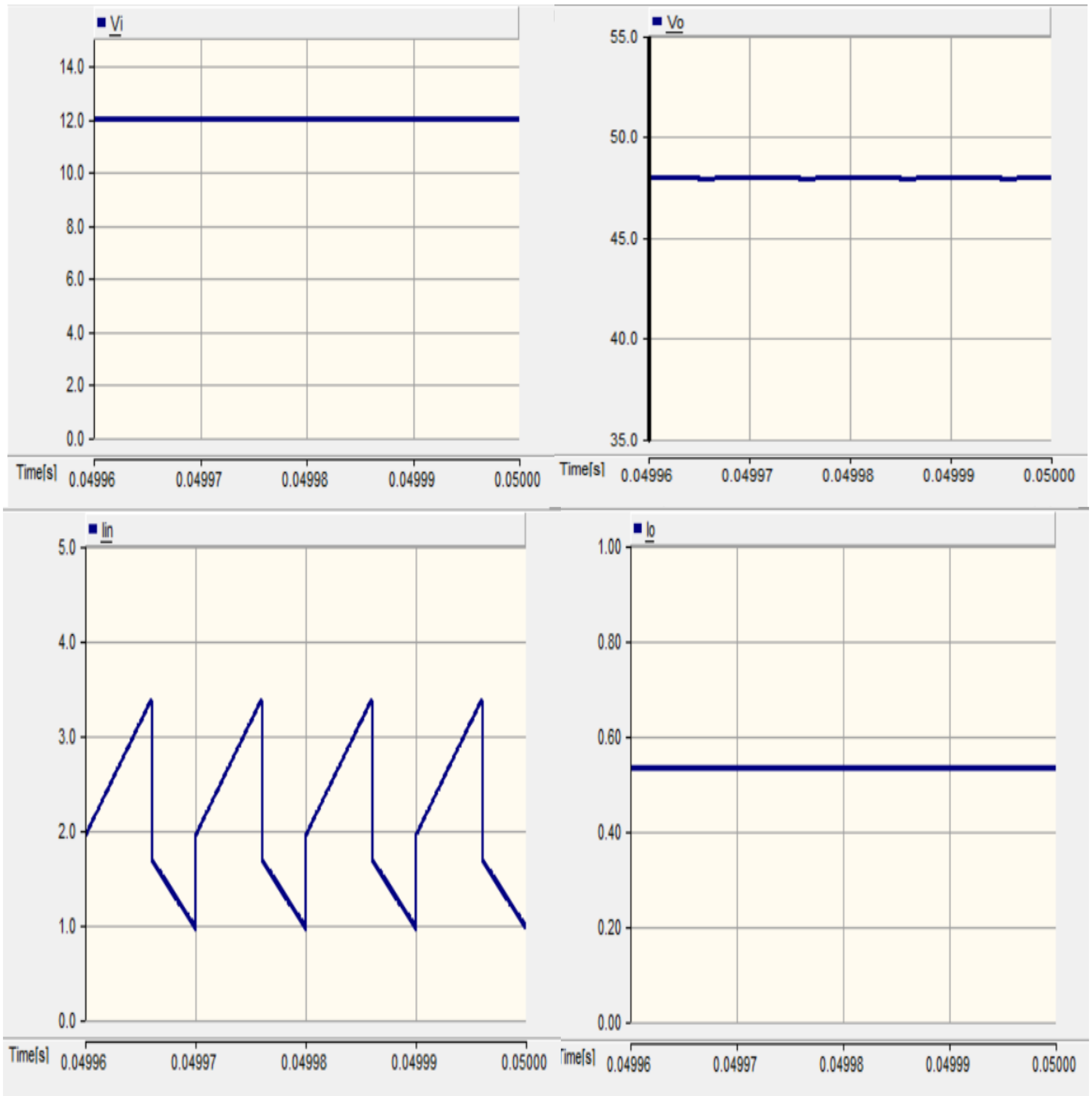

Figure 3.14: Simulation result of converter circuit I: V_{in}, V_o, I_{in}, and voltage I_o.

The currents and voltage waveforms of the two identical inductors L_1 and L_2 are shown in Fig. 3.15. It can be seen that the average values of i_{L1} and i_{L2} are equal. Moreover, the input current is shown in Fig. 3.14 is equal to i_{L1} in off period and is to double for on duration. In addition, from Fig. 3.15, the inductor voltage is equal to $12\ V$, during the switch on and equal to $-18\ V$ during the switch off, which validate the equations (3.1) and (3.2).

In order to demonstrate the significance of selecting the correct value of the inductance, Fig. 3.16 shows the waveforms of the current flowing through the inductors, for inductance value $L = 20\ \mu H$ which is less considering the value set according to the boundary condition

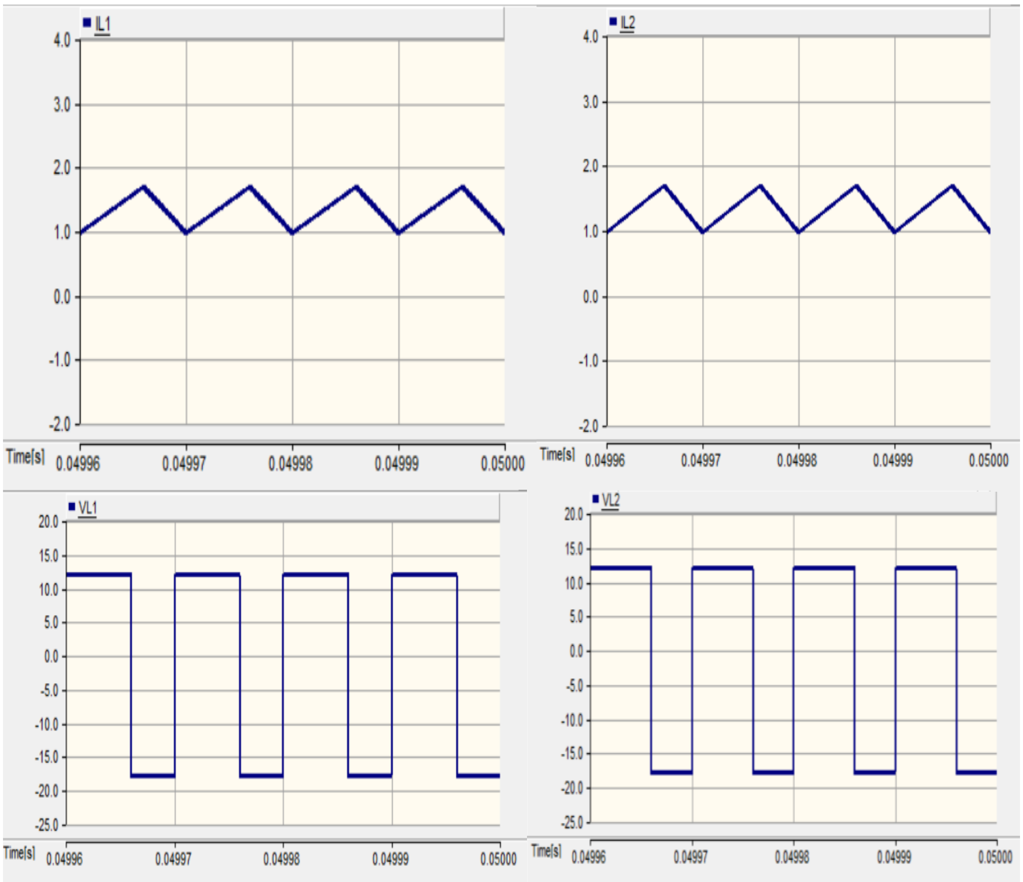

Figure 3.15: Simulation result of converter circuit I: Inductor L_1 current I_{L1}, Inductor L_2 current I_{L2}, Inductor L_1 voltage V_{L1}, Inductor L_2 current V_{L2}.

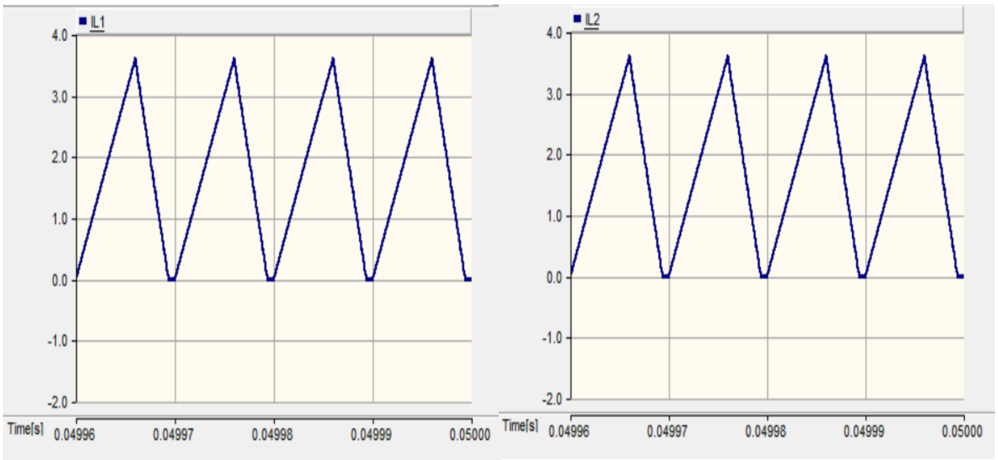

Figure 3.16: Simulation result of converter circuit I in DCM for $L = 20\ \mu H$: Inductor L_1 current I_{L1}, Inductor L_2 current I_{L2}.

Fig. 3.17 shows the voltages stress on the active switches V_{S1} and V_{S2} along with the switch's current i_{S1} and i_{S2} waveforms. The voltage stress is equal to $30\ V$, which is in line with the theoretical fact $(V_o + V_{in})/2$. The voltage stress on the inductor is shown in Fig. 3.18, and also satisfied the theoretical fact expressed in equation (3.7).

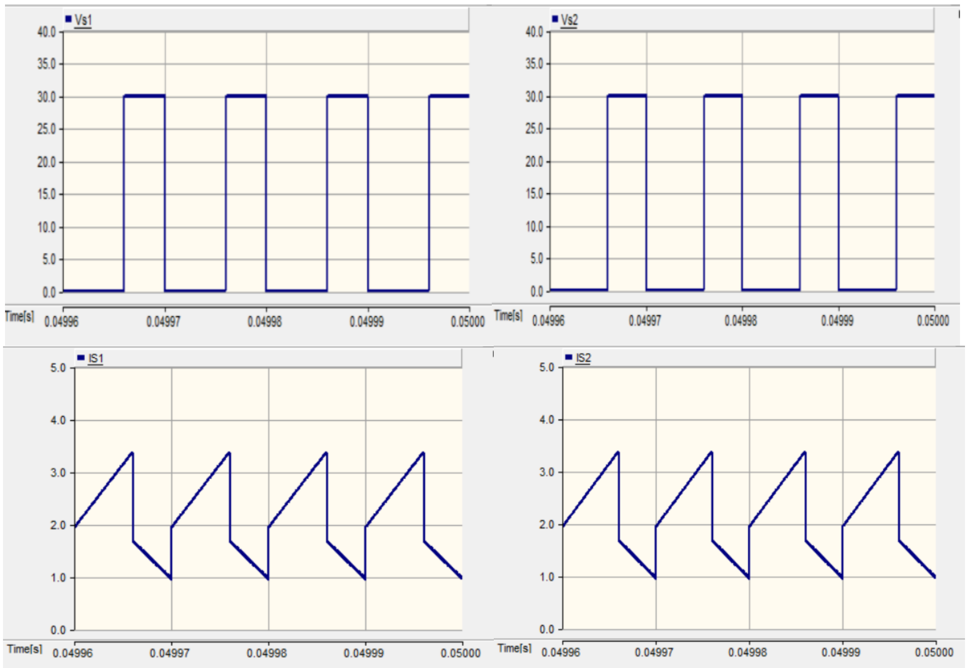

Figure 3.17: Simulation result of converter circuit I: Switch S_1 voltage V_{S1}, Switch S_2 voltage V_{S2}, Switch S_1 current I_{S1}, Switch S_2 current I_{S2}.

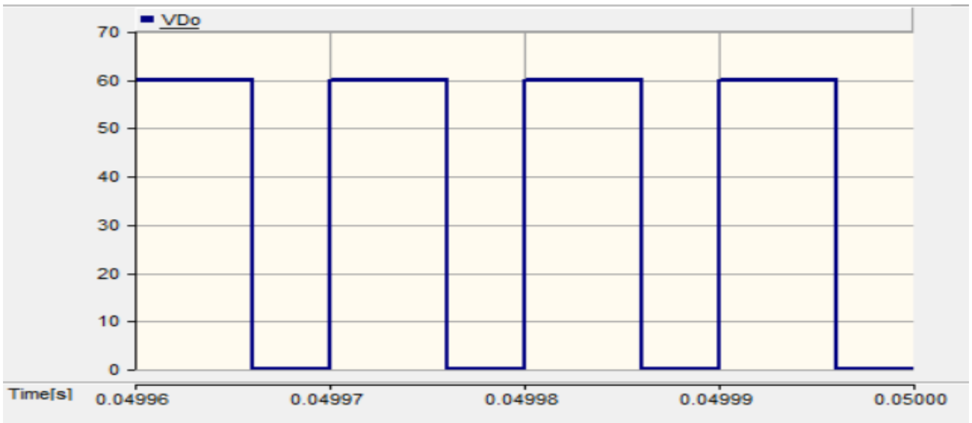

Figure 3.18: Simulation result of converter circuit I: Diode D_1 voltage V_{Do}

3.5.2 Converter circuit II simulation result

For the simulation of converter II shown in Fig. 3.7, the following parameters, have been selected $V_{in} = 12\ V, f_S = 100\ kHz, C_o = 3.33\ \mu F, D = 0.6\ \ and\ R = 130\ \Omega$, for the input voltage, switching frequency, the capacitance of the output capacitor, duty ratio and load resistor. In a similar passion, based on the selected values of the switching frequency f_s and load resistance R the inductor value should be

$$L < \frac{0.02R}{f_s} < 26\ \mu H \quad \text{for DCM} \tag{3.44}$$

$$L > 26\ \mu H \quad \text{for CCM} \tag{3.45}$$

Fig. 3.19 and 3.20 depicted the input/output voltages and inductor currents for different inductance values. As in the previous case the output voltage shown in Fig. 3.19 obeys the converter CCM voltage gain relationship given in equation (3.25). For the inductance value $L = 110\ \mu H$ the converter operates in CCM Fig. 3.19 and operates in DCM Fig. 3.20 for the inductance value $L = 20\ \mu H$, which is in agreement with equations (3.44) and (3.45).

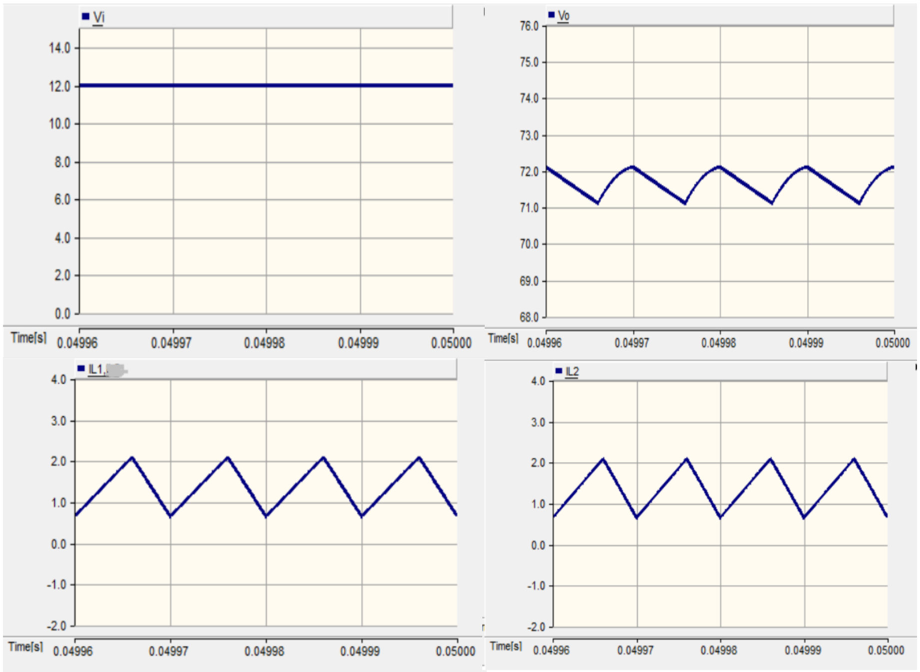

Figure 3.19: Simulation result of converter circuit II in CCM $L = 110\ \mu H$: Input voltage V_{in}, output voltage V_o, inductor L_1 current I_{L1}, inductor L_2 current I_{L2}.

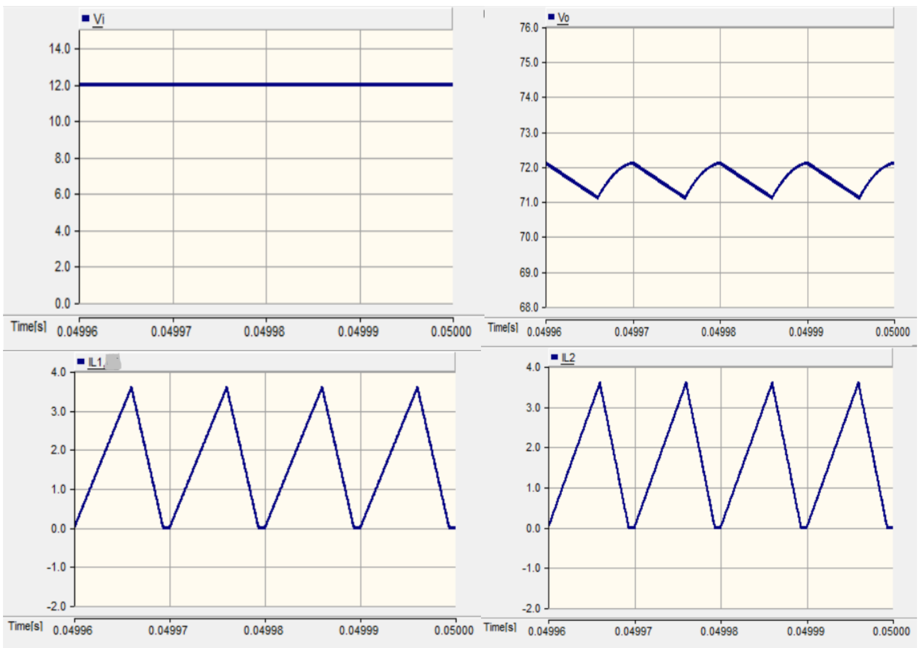

Figure 3.20: Simulation result of converter circuit II in DCM $L = 20\ \mu H$: Input voltage V_{in}, output voltage V_o, inductor L_1 current I_{L1}, inductor L_2 current I_{L2}.

3.6 Chapter Conclusion

This chapter has presented the development and analysis of the two boost converters with large output voltage and relatively reduced stress. The two converter circuits were analysed in both continues conduction mode (CCM) and discontinues conduction mode (DCM), in all the cases the equations governing the voltage gains and the voltage stress across the semiconductor device have been established. For the purpose of comparison, the performance of the two converter circuits was compared with the classical boost converter in terms of voltage gain and voltage stress. To validate the theoretical result a simulation is conducted using PSCAD, and the simulation results satisfy all the theoretical facts.

CHAPTER 4

CONCLUSION AND FUTURE WORK

4.1 Introduction

Here, as the final chapter conclusion and future recommendations are discussed. These recommendations can help in improving the work. This section can also serve as a summary of the salient points made in the thesis.

4.2 Conclusion

This thesis has presented the analysis of power transmission in high step-up dc/dc converter, using two Non-isolated step-up converter. The investigation is performed on Non-isolated converters because of their suitability to many applications. The thesis begins by discussing the basic structure and operating principle of the selected converter circuits. Followed by circuit steady-state analysis in both current continuous conduction mode and discontinuous conduction mode. The significance of the converters has been shown by making a performance comparison with the classical step-up converter. Finally, a simulation is conducted and the result was reported.

In all the cases, during the analysis, ideal circuit components are assumed, with negligible switch's RDS_{ON}, the diode' forward voltage drops and energy storage elements ESR. The first analysed circuit is simple with two identical inductors, two active switches, one output capacitor and single output diode. That makes the circuit less complicated while maintaining the high voltage gain. Similarly, the second converter circuit is slightly more complicated. It is formed by adding two voltage lift circuits containing a diode, inductor and capacitor to converter I. This means there are additional six circuit components. Therefore, the second converter has an increase in the cost of implementation. However, the operation and control are relatively similar to the first circuit. The second circuit provides a significant increased in the voltage gain.

Steady-state analysis of the converters has been performed. Both the converters can operate in continuous current mode and discontinuous current mode. By applying different laws for circuit analysis, together with appropriate equivalent circuits the equations for the converter response are established, including the components voltages and current as well as the output load current and voltage. To obtain the converter CCM and DCM voltage gain the inductor-second property and the output filter capacitor current are used. Boundary conditions between the CCM and DCM are obtained in terms of the inductor time constant. It is shown graphically as well as analytically, that the converter operates in CCM when the time constant is higher than the boundary operation time constant. And it works in DCM when the time constant is less than the boundary operation time constant. This fact help for practical components selection. Further comparison with the classical boost converter, indicated that the converter circuit I increased the voltage gain by 60%. Similarly, converter circuit II increased the voltage gain by almost 140% compared with the voltage gain of the classical step-up converter. Also, both the converters reduce the voltage stress around the semiconductor devices. All these have been shown both analytically and visually through graphs.

Moreover, to complete the analysis, the converter circuits are implemented, to demonstrate the practical applicability and support the theoretical facts. Software-based simulations are commonly used after the design phase to show the system's operation over time. Since its invention, PSCAD has become a popular simulation software for power system and power electronics systems. Therefore, PSCAD / EMTDC-V4.2 is used in this thesis for the simulation. This is a robust software that gives insights and deep understanding of the power electronic circuit. The simulation results show that the theoretical values obtain for the various voltages and currents are the same as those obtained from the simulation. Which further ascertained the effectiveness and accuracy of the analysis. The simulation results also allowed the readers to have a visual understanding of the converter response.

High voltage gain, couple with reduced voltage stress and increased efficiency has been the universal need of dc/dc converter used in modern applications. Step-up converters must be designed with the required specifications to match the increasing demand. Although theoretically it's possible to produce the required high gain from dc/dc converters, yet a more thorough and careful design and analysis is required to make such converters more realistic. Generally, practical dc/dc converters that aimed at producing high voltage gain are affected by ESR of the energy storage elements; the capacitors and inductors, and semiconductor devices. This is in addition to the reverse recovery issue resulting from the necessity of using a high duty cycle ratio.

Literature survey on step-up converter topologies revealed that several topologies have been proposed with the sole aim of providing a high voltage ratio as well as reducing the voltage stress, without necessary using high duty ratio. Majority of the topologies include electrical isolation between the input side and the load. A flyback converter is a typical example of such an isolated converters. Isolated step-up converters are generally less affected by EMI and noise, flexible with positive and negative voltages, however, they are expensive compared to Non-isolated, and required additional coupling circuit and are more suitable for low to high power conversion. Moreover, the use of a transformer in the topology leads to increased voltage stress across the power switches. For this reason, transformer-less step-up converters, that guarantees high voltage gain with relatively low costs and reduced circuit complexity are discussed in this thesis. Power transfer analysis in dc/dc converters is necessary to understand their performance and explore some possible applications. The simulation provided a graphical visualisation of the converter response. Simulation models provide safe and efficient solutions to real-world applications and can, therefore, this thesis also provided an opportunity to study the salient features of the converter and their potential applications.

4.3 Future Work

The thesis focused on the analysis of power transfer in the step-up dc/dc converter. The investigation is limited to mathematical analysis and software simulation. Although the aim of the thesis has been achieved, however, the following recommendations can help in improving future work:

- The analysis should be extended to include a frequency response analysis, stability analysis and optimal components design.
- To further validate the simulation results a prototype should be design
- Also, to bridge the gap between the theory and reality, a real application of the analyzed converters should be performed
- Although the converter explained offers a lot of advantages but the voltage stress is quite large and therefore the future work should be carried out to address this.
- Z-source and soft-switching techniques should also be explored to demonstrate their capabilities.

REFERENCES

Axelrod, B., Berkovich, Y., & Ioinovici, A. (2003). A Family of Isolated Interleaved Boost and Buck. *Proceedings of the 2003 International Symposium on Circuits and Systems, 2003. ISCAS '03.*, *3*(6), 3164–3173.

Axelrod, B, & Berkovich, Y. (2003). Transformaeless dc-dc Converters With a Very High dc Line-To-Load Voltage Ratio. In *Int. Symp. on Circuits and Systems* (Vol. III, pp. 5–8).

Axelrod, Boris, Berkovich, Y., & Ioinovici, A. (2008). Switched-Capacitor/Switched-Inductor Structures for Getting Transformerless Hybrid DC–DC PWM Converters. *IEEE Transaction On Circuit and Systems—I: REGULAR PAPERS*, *55*(2), 687–696.

Baek, J.-W., Ryoo, M. H., Kim, T. J., Yoo, D. W., & Kim, J.-S. (2005). High boost converter using voltage multiplier. In *Proceedings Of IEEE Iecon* (pp. 567–572). IEEE. https://doi.org/10.1109/IECON.2005.1568967

Bryant, B., & Kazimierczuk, M. K. (2007). Voltage-loop power-stage transfer functions with MOSFET delay for boost PWM converter operating in CCM. *IEEE Transactions on Industrial Electronics*, *54*(1), 347–353. https://doi.org/10.1109/TIE.2006.885136

Chen, Y. T., Tsai, M. H., & Liang, R. H. (2005). High-efficiency DC-DC converter with high voltage gain and reduced switch stress. In *Annual Conference of the IEEE Industrial Electronics Society* (pp. 773–802). https://doi.org/10.1049/iet-pel.2013.0589

Cho, J. G., Rim, G. H., & Lee, F. C. (1996). Zero voltage and zero current switching full bridge PWM converter using secondary active clamp. *PESC Record - IEEE Annual Power Electronics Specialists Conference*, *1*, 657–663. https://doi.org/10.1109/PESC.1996.548651

Choi, H. S., & Cho, B. H. (2002). Novel zero-current-switching (ZCS) PWM switch cell minimizing additional conduction loss. *IEEE Transactions on Industrial Electronics*, *49*(1), 165–172. https://doi.org/10.1109/41.982260

Choi, H. S., Kim, J. W., & Cho, B. H. (2002). Novel zero-voltage and zero-current-switching

(ZVZCS) full-bridge PWM converter using coupled output inductor. *IEEE Transactions on Power Electronics*, *17*(5), 641–648. https://doi.org/10.1109/TPEL.2002.802179

Chub, A., Vinnikov, D., Blaabjerg, F., & Peng, F. Z. (2016). A review of galvanically isolated impedance-source DC-DC converters. *IEEE Transactions on Power Electronics*, *31*(4), 2808–2828. https://doi.org/10.1109/TPEL.2015.2453128

Chung, H., Hui, S. Y. R., & Tse, K. K. (1998). Reduction of Power Converter EMI Emission Using Soft-Switching Technique. *IEEE Transection On Electromagnetic Compatibility*, *40*(3), 282–287.

Duarte, C. M. C., & Barbi, I. (1997). A Family ofZVS-PWM Active-Clamping DC-to-DC Converters: Synthesis, Analysis, Design, and Experimentation. *IEEE Transactions on Circuits and Systems*, *44*(8), 698–704.

Forouzesh, M., Yari, K., Baghramian, A., & Hasanpour, S. (2017). Single-switch high step-up converter based on coupled inductor and switched capacitor techniques with quasi-resonant operation. *IET Power Electronics*, *10*(2), 240–250. https://doi.org/10.1049/iet-pel.2015.0923

Garcia, P., Fernandez, L. M., Garcia, C. A., & Jurado, F. (2010). Energy management system of fuel-cell-battery hybrid tramway. *IEEE Transactions on Industrial Electronics*, *57*(12), 4013–4023. https://doi.org/10.1109/TIE.2009.2034173

Garcia, V., Rico, M., Sebastih, J., & Hernando, M. M. (1994). An optimized dc-to-dc converter topology for high-voltage pulse-load applications. In *IEEE Power Electron. Spec. Conf* (Vol. 2, pp. 1413–1421).

Gules, R., & Franco, L. C. (2003). Interleaved Boost Dc-Dc Converter with Large Conversion Ratio. In *IEEE ISIE* (pp. 411–416).

Han, B. M. (2013). Grid-tied power converter for battery energy storage composed of 2-stage DC-DC converter. *IEEE Power and Energy Society General Meeting*, 1–5. https://doi.org/10.1109/PESMG.2013.6672602

Henn, G. A. L., Barreto, L. H. S. C., Oliveira, D. S., & Da Silva, E. A. S. (2008). A novel bidirectional interleaved boost converter with high voltage gain. In *IEEE Applied Power Electronics Conference and Exposition - APEC* (pp. 1589–1594). https://doi.org/10.1109/APEC.2008.4522937

Henrique, L., Colado, S., Antônio, E., Coelho, A., Farias, V. J., Oliveira, J. C. De, … Vieira, J. B. (2005). A Quasi-Resonant Quadratic Boost Converter Using a Single Resonant Network. *IEEE Transaction On Industrial Electronics*, *52*(2), 552–557.

Huber, L., & Jovanovic, M. M. (2000). A Design Approach for Server Power Supplies for Networking Applications. In *IEEE APEC* (pp. 1163–1169).

Ismail, E. H., Al-Saffar, M. A., Sabzali, A. J., & Fardoun, A. A. (2008). A family of single-switch PWM converters with high step-up conversion ratio. *IEEE Transactions on Circuits and Systems I: Regular Papers*, *55*(4), 1159–1171. https://doi.org/10.1109/TCSI.2008.916427

Jahns, T. M., & Dai, H. (2017). The Past , Present , and Future of Power Electronics Integration Technology in Motor Drives. *CPSS Transactions on Power Electronics and Applications*, *2*(3), 197–216.

Jang, Y., & Jovanović, M. M. (2004). New two-inductor boost converter with auxiliary transformer. *IEEE Transactions on Power Electronics*, *19*(1), 169–175. https://doi.org/10.1109/TPEL.2003.820588

Jeon, S. J., Canales, F., Barbosa, P. M., & Lee, F. C. (2002). A primary-side-assisted zero-voltage and zero-current switching three-level DC-DC converter with phase-shift control. In *Conference Proceedings - IEEE Applied Power Electronics Conference and Exposition - APEC*, *2*(c), 641–647. https://doi.org/10.1109/apec.2002.989313

Johnson, S. D., Witulski, A. F., & Erickson, R. W. (1988). Comparison of Resonant Topologies in High-Voltage DC Applications. *IEEE Transactions on Aerospace and Electronic Systems*, *24*(3), 263–274. https://doi.org/10.1109/7.192094

Jovanović, M. M. (1998). A technique for reducing rectifier reverse-recovery-related losses in high-power boost converters. *IEEE Transactions on Power Electronics*, *13*(5), 932–941. https://doi.org/10.1109/63.712314

Kobougias, I. C., & Tatakis, E. C. (2010). Optimal design of a half-wave Cockcroft-Walton voltage multiplier with minimum total capacitance. *IEEE Transactions on Power Electronics*, *25*(9), 2460–2468. https://doi.org/10.1109/TPEL.2010.2049380

Krismer, F., & Kolar, J. W. (2012). Efficiency-optimized high-current dual active bridge converter for automotive applications. *IEEE Transactions on Industrial Electronics, 59*(7), 2745–2760. https://doi.org/10.1109/TIE.2011.2112312

Lee, J. Y., Jeong, Y. S., & Han, B. M. (2011). An isolated DC/DC converter using high-frequency unregulated LLC resonant converter for fuel cell applications. *IEEE Transactions on Industrial Electronics*, *58*(7), 2926–2934. https://doi.org/10.1109/TIE.2010.2076311

Lei, Y., & Pilawa-Podgurski, R. C. N. (2015). A general method for analyzing resonant and soft-charging operation of switched-capacitor converters. *IEEE Transactions on Power Electronics*, *30*(10), 5650–5664. https://doi.org/10.1109/TPEL.2014.2377738

Li, Z., Hoshina, S., Satake, N., & Nogi, M. (2016). Development of DC/DC converter for battery energy storage supporting railway DC feeder systems. *IEEE Transactions on Industry Applications*, *52*(5), 4218–4224. https://doi.org/10.1109/TIA.2016.2582724

Liang, T. J., Lee, J. H., Chen, S. M., Chen, J. F., & Yang, L. S. (2013). Novel isolated high-step-Up DC-DC converter with voltage lift. *IEEE Transactions on Industrial Electronics*, *60*(4), 1483–1491. https://doi.org/10.1109/TIE.2011.2177789

Lin, B.-R., & Hsieh, F. (2007). Soft-Switching Zeta – Flyback Converter With a Buck – Boost Type of Active Clamp. *IEEE Transactions on Industrial Electronics*, *54*(5), 2813–2822.

Lu, D. D. C., Lee, Y. S., & Cheng, D. K. W. (2003). A single-switch continuous-conduction-mode boost converter with reduced reverse-recovery and switching losses. *IEEE Transactions on Industrial Electronics*, *50*(4), 767–776. https://doi.org/10.1109/TIE.2003.814989

Lu, Y., Liu, H., Hu, H., Wu, H., & Xing, Y. (2015). Single-switch high step-up converter with coupled-inductor and built-in transformer. *Proceedings of the 2015 10th IEEE Conference on Industrial Electronics and Applications, ICIEA 2015*, (51177070), 1181–1186. https://doi.org/10.1109/ICIEA.2015.7334286

Luo, F. L. (2001). Six self-lift DC-DC converters, voltage lift technique. *IEEE Transactions on Industrial Electronics*, *48*(6), 1268–1272. https://doi.org/10.1109/41.969408

Luo, F. L., & Ye, H. (2004). Positive Output Multiple-Lift Push – Pull. *IEEE Transaction On Industrial Electronics*, *51*(3), 594–602.

Mao, H., Abu-qahouq, J., Luo, S., Batarseh, I., & Member, S. (2004). Zero-Voltage-Switching Half-Bridge DC – DC Converter With Modified PWM Control Method Hong. *IEEE Transactions on Power Electronics*, *19*(4), 947–958.

Matsuo, H., Harada, K., & Member, S. (1976). The cascade connection of switching regulators. *IEEE Transactions on Industry Applications*, *I*(2), 192–198.

Middlebrook, R. D. (1988). Transformerless DC-to-DC converters with large conversion ratios. *IEEE Trans. Power Electron.*, *3*(4), 484–488.

Naayagi, R. T., Forsyth, A. J., & Shuttleworth, R. (2012). High-power bidirectional DC-DC converter for aerospace applications. *IEEE Transactions on Power Electronics*, *27*(11), 4366–4379. https://doi.org/10.1109/TPEL.2012.2184771

Nymand, M., & Andersen, M. A. E. (2010). High-efficiency isolated boost DCDC converter for high-power low-voltage fuel-cell applications. *IEEE Transactions on Industrial Electronics*, *57*(2), 505–514. https://doi.org/10.1109/TIE.2009.2036024

Papanikolaou, N. P., & Tatakis, E. C. (2004). Active voltage clamp in flyback converters operating in CCM mode under wide load variation. *IEEE Transactions on Industrial Electronics*, *51*(3), 632–640. https://doi.org/10.1109/TIE.2004.825342

Roggia, L., Schuch, L., Baggio, J. E., Rech, C., & Pinheiro, J. R. (2013). Integrated full-bridge-forward dc-dc converter for a residential microgrid application. *IEEE Transactions on Power Electronics*, *28*(4), 1728–1740. https://doi.org/10.1109/TPEL.2012.2214061

Rotman, E., & Ben-Yaakov, S. S. (2013). Rapid push pull resonant charger for high power, high voltage applications using low input voltage. *2013 IEEE Energy Conversion Congress and Exposition, ECCE 2013*, 2325–2332. https://doi.org/10.1109/ECCE.2013.6646998

Senthil Kumar, S., Siva Ramkumar, M., Amudha, A., Balachander, K., & Emayavaramaban, G. (2018). Cascade cockcroft-walton voltage multiplier applied to transformerless high step-up DC-DC converter. *Journal of Advanced Research in Dynamical and Control Systems*, *10*(5 Special Issue), 1082–1088. https://doi.org/10.1109/TIE.2012.2188255

Siwakoti, Y. P., Blaabjerg, F., Loh, P. C., & Town, G. E. (2014). High-voltage boost quasi-Z-source isolated DC/DC converter. *IET Power Electronics*, *7*(9), 2387–2395. https://doi.org/10.1049/iet-pel.2013.0845

Siwakoti, Y. P., Peng, F. Z., Blaabjerg, F., Loh, P. C., & Town, G. E. (2015). Impedance-source networks for electric power conversion Part I: A topological review. *IEEE Transactions on Power Electronics*, *30*(2), 699–716. https://doi.org/10.1109/TPEL.2014.2313746

Song, T. T., Huang, N., & Ioinovici, A. (2005). A family of zero-voltage and zero-current-switching (ZVZCS) three-level DC-DC converters with secondary-assisted regenerative passive snubber. *IEEE Transactions on Circuits and Systems I: Regular Papers*, *52*(11), 2473–2481. https://doi.org/10.1109/TCSI.2005.853911

Song, W., & Lehman, B. (2004). Dual-bridge DC-DC converter: A new topology characterized with no deadtime operation. *IEEE Transactions on Power Electronics*, *19*(1), 94–103. https://doi.org/10.1109/TPEL.2003.820600

Song, W., & Lehman, B. (2007). Current-fed dual-bridge dc-dc converter. *IEEE Transactions on Power Electronics*, *22*(2), 461–469. https://doi.org/10.1109/TPEL.2006.889927

Steigerwald, R. L., Doncker, R. W. D., & Kheraluwala, M. H. (1996). A Comparison of High-Power DC-DC Soft-Switched Converter Topologies Robert. *IEEE Transactions on Industrial Electronics, 32*(5), 1139–1145.

Sun, J., Ding, X., Nakaoka, M., & Takano, H. (2000). Series resonant ZCS-PFM DC-DC converter with multistage rectified voltage multiplier and dual-mode PFM control scheme for medical-use high-voltage X-ray power generator. *IEE Proceedings: Electric Power Applications*, *147*(6), 527–534. https://doi.org/10.1049/ip-epa:20000711

Thummala, P., Maksimovic, D., Zhang, Z., & Andersen, M. A. E. (2016). Digital Control of a High-Voltage (2.5 kV) Bidirectional DC-DC Flyback Converter for Driving a Capacitive Incremental Actuator. *IEEE Transactions on Power Electronics*, *31*(12), 8500–8516. https://doi.org/10.1109/TPEL.2016.2520497

Torrico-bascope, G. V., Vasconcelos, S. A., Torrico-bascope, R. P., Antunes, F. L. M., Jr., D. S. de O., & Branco, C. G. C. (2006). A High Step-Up DC-DC Converter Based on Three-State Switching. In *IEEE ISIE 2006,* (pp. 998–1003).

Tseng, K. C., & Liang, T. J. (2004). Novel high-efficiency step-up converter. In *IEE Proc.-Electr. Power Appl.* (Vol. 151, pp. 182–190). https://doi.org/10.1049/ip-epa

Vinnikov, D., & Roasto, I. (2011). Quasi-Z-Source-based isolated DC/DC converters for distributed power generation. *IEEE Transactions on Industrial Electronics*, *58*(1), 192–201. https://doi.org/10.1109/TIE.2009.2039460

Wai, R. J., & Dua, R. Y. (2005). High-efficiency DC/DC converter with high voltage gain. In *IEEE Elect. Power Appl.* (Vol. 152, pp. 793–802). https://doi.org/10.1049/ip-epa

Wai, Rong Jong, Lin, C. Y., Lin, C. Y., Duan, R. Y., & Chang, Y. R. (2008). High-efficiency power conversion system for kilowatt-level stand-alone generation unit with low input voltage. *IEEE Transactions on Industrial Electronics*, *55*(10), 3702–3714. https://doi.org/10.1109/TIE.2008.921251

Wang, C. (2006). Novel Zero-Voltage-Transition PWM DC – DC Converters. *IEEE Transactions on Industrial Electronics*, *53*(1), 254–262.

Wang, C. M. (2008). A novel ZCS-PWM flyback converter with a simple ZCS-PWM commutation cell. *IEEE Transactions on Industrial Electronics*, *55*(2), 749–757. https://doi.org/10.1109/TIE.2007.911917

Williams, B. W. (2013). DC-to-DC converters with continuous input and output power. *IEEE Transactions on Power Electronics*, *28*(5), 2307–2316. https://doi.org/10.1109/TPEL.2012.2213272

Wilson, T. G. (1992). The evolution of power electronics. *IEEE International Symposium on Industrial Electronics*, *15*(3), 1–9. https://doi.org/10.1109/ISIE.1992.279629

Wu, T. F., Lai, Y. S., Hung, J. C., & Chen, Y. M. (2008). Boost converter with coupled inductors and buck-boost type of active clamp. *IEEE Transactions on Industrial Electronics*, *55*(1), 154–162. https://doi.org/10.1109/TIE.2007.903925

Wu, T. F., & Yu, T. H. (1998). Unified approach to developing single-stage power converters. *IEEE Transactions on Aerospace and Electronic Systems*, *34*(1), 211–223. https://doi.org/10.1109/7.640279

Wu, X., Zhang, J., Ye, X., & Qian, Z. (2008). Analysis and derivations for a family ZVS converter based on a new active clamp ZVS cell. *IEEE Transactions on Industrial Electronics*, *55*(2), 773–781. https://doi.org/10.1109/TIE.2007.907675

Yan, L., & Lehman, B. (2005). An integrated magnetic isolated two-inductor boost converter: Analysis, design and experimentation. *IEEE Transactions on Power Electronics*, *20*(2), 332–342. https://doi.org/10.1109/TPEL.2004.843004

Yan, L., Qu, D., & Lehman, B. (2003). Integrated magnetic full wave converter with flexible output inductor. *IEEE Transactions on Power Electronics*, *18*(2), 670–678. https://doi.org/10.1109/TPEL.2003.809357

Yang, L. S., Liang, T. J., & Chen, J. F. (2009). Transformerless DC-DC converters with high step-up voltage gain. *IEEE Transactions on Industrial Electronics*, *56*(8), 3144–3152. https://doi.org/10.1109/TIE.2009.2022512

Yao, C., Ruan, X., Wang, X., & Tse, C. K. (2011). Isolated buck-boost dc/dc converters suitable for wide input-voltage range. *IEEE Transactions on Power Electronics*, *26*(9), 2599–2613. https://doi.org/10.1109/TPEL.2011.2112672

Zhang, M. T., Jiang, Y., Lee, F. C., & Jovanovic, M. M. (1995). Single-phase three-level boost power factor correction converter. In *Conference Proceedings - IEEE Applied Power Electronics Conference and Exposition - APEC*, *1*, 434–439. https://doi.org/10.1109/apec.1995.468984

Zhao, B., Song, Q., Liu, W., & Sun, Y. (2014). Overview of dual-active-bridge isolated bidirectional DC-DC converter for high-frequency-link power-conversion system. *IEEE Transactions on Power Electronics*, *29*(8), 4091–4106. https://doi.org/10.1109/TPEL.2013.2289913

Zhao, B., Yu, Q., Leng, Z., & Chen, X. (2012). Switched Z-source isolated bidirectional dc-dc converter and its phase-shifting shoot-through bivariate coordinated control strategy. *IEEE Transactions on Industrial Electronics*, *59*(12), 4657–4670. https://doi.org/10.1109/TIE.2011.2181136

Zhao, Q., & Lee, F. C. (2003). High-efficiency, high step-up dc-dc converters. *IEEE Transactions on Power Electronics*, *18*(1 I), 65–73. https://doi.org/10.1109/TPEL.2002.807188

Zhou, D., Pietkiewicz, A., & Cuk, S. (1999). A Three-Switch High-Voltage Converter. *IEEE Transactions On Power Electronics*, *14*(1), 177–183.

YAKIN DOĞU ÜNİVERSİTESİ

ETHICAL APROVAL DOCUMENT

Date: ___/___/____

To the **Graduate School of Applied Sciences**

The research project titled "Analysis of Power Transmission in high Step-up Dc-Dc converter"

has been evaluated. Since the researcher(s) will not collect primary data from humans, animals, plants or earth, this project does not need to go through the ethics committee.

Title: Analysis of Power Transmission in high Step-up DC-DC converter

Name Surname: Prof. Dr. Ebrahim Babaei

Signature:

Role in the Research Project: Supervisor

Title:

Name Surname:

Signature:

Role in the Research Project: Co-Supervisor

Thesis Alaa

INBOX | NOW VIEWING: NEW PAPERS ▼

Submit File

Online Grading Report | Edit assignment settings | Email non-submit

AUTHOR	TITLE	SIMILARITY	GRADE	RESPONSE	FILE	PAPER ID	DATE
Alaa Abdullah	Abstract	0%	--	--		1233835933	13-Dec-2019
Alaa Abdullah	conclusion	0%	--	--		1233051351	12-Dec-2019
Alaa Abdullah	Chapter 3	4%	--	--		1233836724	13-Dec-2019
Alla Abdullah	Chapter 1	6%	--	--		1233836098	13-Dec-2019
Alaa Abdullah	Chapter 2	11%	--	--		1233836385	13-Dec-2019
Alaa Abdullah	complete	15%	--	--		1233837313	13-Dec-2019

Asst. Prof. Dr. Parvaneh Esmaili